

IMAGING BIOLOGICALLY-BASED CLATHRATE HYDRATE INHIBITORS

by

Raimond Gordienko

A thesis submitted to the Department of Biology
in conformity with the requirements for
the degree of Master of Science

Queen's University
Kingston, Ontario, Canada

August, 2009

Copyright © Raimond Gordienko, 2009

Abstract

The unscheduled formation of gas hydrate plugs in oil and gas pipelines, which can lead to serious mechanical and personnel damage, is a problematic issue in the petroleum industry. Traditionally, thermodynamic inhibitors such as methanol have been used to control the formation of gas hydrates, but due to the large expenses and ecological risks associated with its use there is increased interest in the use of alternative hydrate inhibitors. They include kinetic inhibitors (KIs) and antiagglomerants (AAs) and as their names imply, function by interfering with the kinetics of hydrate formation and hydrate agglomeration.

Recently, antifreeze proteins (AFPs) have shown to inhibit hydrates and have been proposed as hydrate inhibitors. Normally, AFPs function to protect the tissues of various organisms during freezing conditions. Initially they were found in polar fish, and were later recognized in insects, plants and microorganisms. AFPs are thought to function by lowering the freezing point of water through an adsorption-inhibition mechanism.

This thesis has shown that antifreeze proteins (AFPs) are able to modify the crystal morphologies of structure II (sII) tetrahydrofuran (THF) similarly to the KI poly-N-vinylpyrrolidone (PVP) by adhering to the hydrate surface and inhibiting crystal growth. The AFPs were also tested on a high-pressure sII methane/ethane/propane hydrate and proved to have superior hydrate inhibition to PVP. Yet, the expense of purifying AFPs makes them impractical for industrial purposes, thus investigations into the use of cold-adapted bacteria as hydrate inhibitors proved that isolates capable of adsorbing to THF hydrate showed the most effective THF hydrate inhibition. These findings suggest a potential for the future development of biologically-based hydrate inhibitors.

Acknowledgements

Virginia K. Walker, your unparalleled enthusiasm, cheerfulness and knowledge as a supervisor and friend has been a source of inspiration throughout this thesis and my time at Queen's, I sincerely thank you.

I thank my committee members Ken Ko, Heather Jamieson and John Ripmeester for their time and advice throughout the progression of my thesis.

Members of the Walker Lab, former and current; Julie Choi, Emily Huva, Niraj Kumar, Shaun Nowickyj, Nikki Philbrook, Tara Vanderveer, Sandra Wilson and Suzy Wu, additionally, department members; Linda Cameron, Josh Powles, Grace Tharmarajah, Matt Vankoughnett and Tara Zamin, my thanks to all your assistance and friendship, you have made every day at work and out enjoyable and memorable.

I also thank NRC faculty Dr. Hiroshi Ohno, Rajneesh Kumar and Robin Susilo as well Sherry Gauthier and Adam Middleton from Queen's Biochemistry for their kind assistance and advice throughout my thesis.

I thank my friends Andrew Palombella, Scott Robson and Andrew Seniuk for their shared conversation and experiences here in Kingston, I will never forget our times together.

To my family, for all their care and support throughout all the years of life and to my mother, who has been my guiding light.

Co-Authorship

Chapters 2 and 3. Dr. Hiroshi Ohno assisted with the high-pressure gas mix hydrate work.

Appendix A. Dr. Robin Susilo assisted with the high-pressure methane hydrate work.

Table of Contents

| | |
|----------------------------|------|
| Abstract..... | ii |
| Acknowledgements..... | iii |
| Co-Authorship..... | iv |
| Table of Contents..... | v |
| List of Figures..... | viii |
| List of Tables..... | viii |
| List of Abbreviations..... | ix |

Chapter 1 Introduction and Literature Review

| | |
|--|----|
| Clathrate Hydrates..... | 1 |
| Properties and Varieties..... | 1 |
| Hydrates in Industry..... | 2 |
| Hydrate Plugs..... | 3 |
| Preventing Hydrate Growth..... | 4 |
| Thermodynamic Inhibitors..... | 4 |
| Chemical Kinetic Inhibitors..... | 5 |
| Antifreeze Proteins..... | 6 |
| AFP Diversity..... | 7 |
| AFP Activities..... | 11 |
| Applications of AFPs..... | 11 |
| Cold-Adapted and Freeze-Tolerant Bacteria..... | 12 |
| Bacterial AFPs..... | 13 |
| Biotechnological Applications..... | 14 |
| Research Objectives..... | 15 |
| References..... | 16 |

Chapter 2 Towards A Green Hydrate Inhibitor: Imaging AFPs on Clathrate Hydrates

| | |
|----------------------------|----|
| Abstract | 26 |
| Introduction..... | 27 |
| Materials and Methods..... | 28 |
| Results..... | 33 |
| Discussion | 36 |
| References..... | 46 |

Chapter 3 Tetrahydrofuran Hydrate Inhibition using Cold-Adapted Bacteria

| | |
|------------------------------|----|
| Abstract | 48 |
| Introduction..... | 49 |
| Materials and Methods..... | 50 |
| Results and Discussion | 52 |
| References..... | 56 |

Chapter 4 General Discussion

| | |
|---|----|
| 4.1. AFP binding and hydrate inhibition..... | 62 |
| 4.2. Cold-adapted bacteria and hydrate inhibition | 67 |
| 4.3. Concluding comments | 68 |
| References..... | 70 |
| Summary | 73 |

Appendix A AFPs and sI Methane Hydrate

| | |
|--------------------------|----|
| Abstract | 74 |
| Introduction..... | 74 |
| Methods and Results..... | 75 |
| Discussion..... | 76 |
| References..... | 77 |

Appendix B AFP Adsorption studies with Amorphous Silica and Quartz

| | |
|------------------------------|----|
| Abstract | 79 |
| Introduction..... | 80 |
| Materials and Methods..... | 80 |
| Results and Discussion | 82 |
| References..... | 84 |

Appendix C Bacterial standard curves 88

List of Figures

| | | |
|------------|--|----|
| Fig. 1.1 | Common clathrate hydrate structures..... | 23 |
| Fig. 1.2 | Low dosage hydrate inhibitors..... | 24 |
| Fig. 1.3 | Structural varieties of AFPs..... | 25 |
| Fig. 2.1 | Typical bioreactor DO and OD ₆₀₀ trends for <i>E. coli</i> BL21 expressing Recombinant AFPs..... | 39 |
| Fig. 2.2 | Purified recombinant proteins on a 12% SDS-PAGE gel | 40 |
| Fig. 2.3 | Fluorescence in AFP-adsorbed polycrystalline THF hydrate..... | 41 |
| Fig. 2.4 | Levels of AFP adsorption into THF hydrate..... | 42 |
| Fig. 2.5 | Single THF hydrate crystals grown under various additives and conditions..... | 43 |
| Fig. 2.6 | Pressure summary of sII mixed gas hydrate with various additives..... | 44 |
| Fig. 3.1 | Bacterial cultures with added THF: pre and post Triton X-100 addition..... | 58 |
| Fig. 3.2 | Levels of bacterial adsorption into THF hydrate..... | 59 |
| Fig. 3.3 | THF hydrate growth rate in various bacterial cultures..... | 60 |
| Fig. 3.4 | sII mixed gas hydrate gas uptake with 10% TSB and <i>P. putida</i> UW4..... | 61 |
| Fig. A.1 | Pressure trends for methane hydrate with various additives..... | 78 |
| Fig. B.1 | Typical QCM-D frequency and dissipation trends..... | 86 |
| Fig. B.2.A | Protein elution from quartz with 0.1 M Tris/HCl (pH 8)..... | 87 |
| Fig. B.2.B | Protein elution from quartz with 0.1 M Tris/HCl (pH 1.3)..... | 88 |

List of Tables

| | | |
|------------|---|----|
| Table B.1. | Summary of changes in QCM-D frequency and dissipation using various additives..... | 85 |
|------------|---|----|

List of Abbreviations

| | |
|---------------|--|
| AA | antiagglomerant |
| AFGP | antifreeze glycoprotein |
| AFP | antifreeze protein |
| ANP | anti-nucleating proteins |
| CfAFP | <i>Choristoneura fumiferana</i> antifreeze protein |
| GFP | green fluorescent protein |
| INP | ice nucleating protein |
| IRI | ice-recrystallization inhibition |
| Da | Dalton |
| KHI | kinetic hydrate inhibitor |
| KI | kinetic Inhibitor |
| LDHI | low-dosage hydrate inhibitors |
| LpAFP | <i>Lolium perenne</i> antifreeze protein |
| NMR | Nuclear magnetic resonance |
| PVCap | poly-N-vinylcaprolactam |
| PVP | poly-N-vinylpyrrolidone |
| sbwAFP | spruce budworm antifreeze protein |
| sH | structure H |
| sI | structure I |
| sII | structure II |
| TH | thermal hysteresis |
| THF | tetrahydrofuran |
| TmAFP | <i>Tenebrio molitor</i> antifreeze protein |
| wfAFP | winter flounder antifreeze protein |

| | |
|-------------|--|
| IPTG | isopropyl β -D-1-thiogalactopyranoside |
| DO | dissolved oxygen |
| OD | optical density |
| nGas | moles of gas consumed |

Chapter 1

Introduction and Literature Review

1. Clathrate Hydrates

A. Properties and Varieties

Clathrate hydrates are solid crystalline, ice-like inclusion compounds, where water forms a hydrogen-bonded framework of relatively large polyhedral cavities that are occupied by individual gases or gas mixtures.¹ Sir Humphrey Davy first described them in 1810 when he cooled an aqueous chlorine solution below 9°C and it became a solid.² Presently there are more than 100 known chemical species that can be enclathrated by water, nonetheless most clathrate hydrates can be divided into three commonly observed crystal structures: cubic structure I (sI), cubic structure II (sII) and hexagonal structure H (sH), each differing in their cage size and unit cell composition (Fig. 1.1).³ sI possesses two cavities, one is pentagonal dodecahedral (denoted as 5^{12} , indicating a cage lattice composed of 12 pentagons) and a tetracaidecahedral cavity $5^{12} 6^2$ (composed of 12 pentagons and 2 hexagons). Similarly, sII is produced from two cavities, a 5^{12} and a hexacaidecahedral cavity (16-hedra) designated as $5^{12} 6^4$. Lastly, sH, containing the largest cages of the three,⁴ is denoted as $5^{12} 6^8$.

The guest molecule dictates which type of crystal structure will form. For example, small guest molecules such as methane and ethane will commonly form sI, while medium sized guests like propane will form sII, and larger molecules like pentanes, hexanes and heptanes can form sH.⁵ The guest molecule also dictates the conditions required for hydrate formation. Normally, all hydrates require relatively low temperature ranges of 2 to 12°C to form. Some hydrocarbon-based hydrates (formed from natural oil and gas deposits), apart from low temperatures, require

higher pressures, usually ten to one hundred times the atmospheric pressure to successfully form.⁵ Conversely, some non-naturally occurring hydrates of ethylene oxide (sI), cyclopentane (sII) or tetrahydrofuran (THF, sII) form under standard atmospheric pressure, circumventing the need for high-pressure equipment, thus they are commonly used as popular analogues for the study of natural gas hydrates.⁶ Hydrate decomposition occurs when there is a deviation of either pressure or temperature (or both) from the normal hydrate forming range, causing the hydrogen bonds in the water cage to break and subsequently releasing the guest molecule.⁷

B. Hydrates in Industry

Apart from their interesting chemical properties, hydrates have significant roles in the energy sector, primarily energy recovery, storage and transportation, as well as safety and flow assurance. It is estimated that there is an extensive reservoir of natural gas trapped inside clathrate hydrates on the ocean bottom and in arctic permafrost; some estimates predict $10,000 \times 10^{12}$ kg of methane, which corresponds to 53% of all currently known fossil fuel reserves on the planet.⁸ Presently the costs associated with extracting natural gas from these reserves are excessive, but it is nevertheless predicted that with more sophisticated technologies and equipment, energy recovery will begin in less than two decades.⁹ Additionally the extraction, containment and transport of natural gas from remote areas is both expensive and potentially hazardous.¹⁰ An alternative to conventional methods of gas transport via pipeline or conversion to a liquid through pressurization is to trap the gas in hydrate form.¹¹ Advantages of this method include increased stability since hydrates have been found to be stable for up to 15 days if stored at -15°C at atmospheric pressure with little gas lost.¹² It is also less expensive; one study showed a 24% cost saving in transporting natural gas in hydrate form as opposed to liquid form.¹³

Inherently, there are still some difficulties associated with this method. They include the hydrating rate (rate of hydrate formation at the gas/liquid interface), which can be very slow at times, and storage capacity (amount of hydrocarbon that can be economically stored as hydrate).¹⁴

C. Hydrate Plugs

While gas hydrates will undoubtedly play a significant role in the future of energy, their unscheduled formation in oil and gas pipelines is a continuing threat to flow assurance.¹⁵ In the early 1930's, when the oil and gas industry was growing rapidly in the United States, pipeline plugging was thought to be due to ice formation. However, Hammerschmidt (1934) revealed that gas hydrates were the underlying cause of the problem.¹⁶

During the past decade there has been a gradual shift towards more deep-water oil and gas exploration and production. As a consequence of the lower temperatures and higher pressure in these depths, hydrate formation is commonly observed.⁵ The solid mass can build up in tubing, wellheads, manifolds, valves and pipelines, essentially congesting them and halting production, sometimes for months.¹⁷ If these plugs are decomposed too quickly, the massive release of gas can lead to an increase in pressure in the lines, which can cause devastating damage to both the pipeline itself and surface facilities. The world's most notorious offshore oil disaster was in 1988, when the Piper Alpha rig in the North Sea experienced a sudden rise in pressure as a result of decomposing methane hydrate. This led to a surface blowout that killed 167 crewmembers and destroyed the rig; with a total cost of (US) \$3.4 billion.¹⁸ Additionally, when they detach from pipe walls, the hydrate plugs travel with pressure gradients up to 300 km/h, and can erupt from pipe elbows. One such incident led to the loss of three lives and (US)

\$7 million in costs.¹⁹ Limiting the formation of hydrate plugs is essential for the safety of personnel and flow assurance in oil and gas platforms.

D. Preventing Hydrate Growth

A fundamental understanding of the process of hydrate growth is necessary prior to designing preventative strategies for hydrate inhibition. Initial hydrate formation involves an induction period, often termed as nucleation, where thermodynamically stable hydrate crystals form and are able to successfully grow.²⁰ Nucleation is a stochastic process that is difficult to model and predict, with a multitude of influencing factors.²¹ Important elements involved in hydrate nucleation and growth include the degree of supercooling (defined as $\Delta T = T_{eq} - T_{exp}$, where T_{eq} is the equilibrium hydrate formation temperature at a given pressure and T_{exp} is the experimental temperature), pressure (in natural gas hydrates), heat and mass transfer, mixing, presence of nucleating promoters (particles like dust or structures such as pipeline walls) and the “history” of the solution (a phenomenon known as memory, where accelerated hydrate nucleation occurs after a brief melt).^{3,7,22} Hydrate inhibitors are used to interfere with some of these processes, and are essential for controlling hydrate formation in the oil and gas industry.

E. Thermodynamic Inhibitors

Thermodynamic inhibitors are the most widely used hydrate inhibitors and include polar compounds such glycols and alcohols as well as water-soluble salts.¹⁹ They are believed to function by increasing the competition for water via hydrogen bonding (glycols, alcohols) and Coulombic forces (salt ions). This creates a shift in the hydrate formation phase boundary and ultimately leads to an increase in driving force required to form the hydrate.²³ Although

methanol is one of the most effective and widely used thermodynamic inhibitors in the gas and oil industry, there are many problems associated with its use. Firstly, methanol is very expensive. At \$0.56/L, a small two-well oil field may use more than 20,000 kg of methanol per day, and over the span of one year the costs can add to over (US) \$5 million. It is also estimated that annual worldwide costs for using methanol solely for hydrate inhibition amounts to over (US) \$200 million.²⁴ Secondly, methanol is a toxic and highly flammable alcohol, and thus transporting and handling the large quantities required poses a significant safety concern for personnel and the environment.²⁴ Finally, methanol ultimately contaminates the recovered hydrocarbons, which then require downstream processing, further adding to the time and costs.²⁵ Therefore, the considerable economic, environmental and personnel risks associated with the use of thermodynamic inhibitors like methanol have led to the development of alternative inhibitors.

F. Chemical Kinetic Inhibitors

A more recently introduced class of hydrate inhibitors are the low-dosage hydrate inhibitors (LDHIs) (Fig. 1.2). They are subdivided into kinetic hydrate inhibitors (KHIs) and antiagglomerants (AAs) depending on how they act on hydrate crystal growth. KHIs are water-soluble, generally non-toxic polymers that are active at low concentrations (down to 0.5-3 wt% in water), and examples include poly-N-vinylpyrrolidone (PVP), poly-N-vinylcaprolactam (PVCap) and terpolymers like VC-713.²⁶ Mechanistically, KHIs function by delaying hydrate nucleation as well as decreasing crystal growth rate by adsorbing to the surface of the growing crystal, creating local curvature on the crystal surface.²⁷ This mechanism may be analogous to the interactions of AFPs with ice.²⁸ Although KHIs do offer a suitable solution to the problems associated with thermodynamic inhibitors, at high rates of subcooling (approximately 15°C)

hydrate formation becomes inevitable, regardless of the concentration of KHIs.²⁹ This limits the use of KHIs to applications where subcooling is mild. Additionally, although KHIs are effective in low amounts, the average cost is (US) \$5-6/L; this leads to the same operational expenditure as using methanol.²⁵

Antiagglomerants are amphiphathic surface-active molecules with residues that interact with both water and oil.²⁹ There are a great variety of AA structures, some industrially effective molecules include oligo-vinyl caprolactams with alkylthioether end- groups as well as oligo-N,N-diethylacrylamides. The amphiphathic nature of AAs permits the hydrate crystals to be suspended in the condensate, preventing the further congregation of crystals into large masses.²⁹ Unlike KHIs, they do not prevent hydrate formation, instead they surround the already present hydrate masses, allowing for smaller, more manageable hydrate crystals to travel through pipelines in a slurry form. Additionally AAs can endure higher rates of subcooling than KHIs, up to 20°C.²⁵ AA efficiency is nonetheless compromised when the watercut is more than 30-40%, this leads to a slurry so thick that AA addition interferes with the suspension's flow. Thus, AAs are generally used in combination with methanol to decrease amounts of injected methanol and accelerate the restart of wells.¹⁷

Currently, the search for an inexpensive, effective, and environmentally-safe hydrate inhibitor system is an ongoing process that is crucial for the future of oil and gas exploration and development. Recent research in our lab has suggested that antifreeze proteins may act similarly to more traditional chemical inhibitors and may be a novel inhibitor for hydrates.³⁰

2. Antifreeze Proteins

Antifreeze proteins (AFPs) are found in a diversity of organisms exposed to low temperatures (Fig. 1.3). AFPs can act in freeze-resistant species to lower the freezing point and

in freeze-tolerant organisms to prevent cellular damage as a result of freezing. AFPs function to lower the freezing point below the equilibrium temperature of ice formation, essentially causing a separation between the melting and freezing point, a phenomenon known as thermal hysteresis (TH).²⁸ Although there may be large structural and thermal hysteretic differences between AFPs from different species, they all possess the common ability to bind to ice, and by doing so, they limit water-accessibility on the ice surface, causing the ice to grow in a curved fashion around the adsorbed protein, leading to a non-colligative and thermodynamically unfavorable growth process known as the Kelvin effect.³¹

A. AFP Diversity

Fish AFPs

In the late 1950s, the Canadian scientist P.F Scholander described two species of marine fish that withstood subzero temperatures and hypothesized they contained an internal antifreeze component apart from salts.³² Soon afterwards, research by DeVries and his colleagues led to the discovery of what is known today as antifreeze proteins and glycoproteins.³³ Antifreeze glycoproteins (AFGPs) exist in at least eight structurally-related forms, divided according to their molecular masses which range from 2.6 kDa to 33.7 kDa. They have a maximum thermal hysteresis of 1.2°C (at 40 mg/ml) and comprise a large fraction of blood serum protein of Antarctic notothenioids and Arctic cod. They contain a number of Ala-Ala-Thr repeats along with a β -d-galactosyl-(1→3)- α -N-acetyl-d-galactosamine disaccharide joined to the Thr residues.³⁴ Interestingly, while they are found in unrelated notothenioids, their sequences remain highly conserved with an occasional Arg replacing a Thr, as a result it lacks a disaccharide at that position. It is believed that the polysaccharide moieties are involved in ice-binding via the polar

hydroxyl groups and can be incorporated into the ice-crystal, explaining their ability to permanently adsorb themselves to ice. Additionally, their removal from the polypeptide backbone eliminates any antifreeze activity, underscoring their importance in the adsorption to ice in AFGPs.³⁵

Type I AFP is one of the best characterized of the fish AFPs. It occurs naturally during winter months in the blood plasma of fish from three taxonomic groups: Scorpaeniformes, Perciformes and Pleuronectiformes.³⁶ The latter includes species like the winter flounder (*Pleuronectes americanus*) whose Type I AFP is well characterized as a single α -helix, alanine-rich, 3.3 kDa amphipathic molecule with a maximum TH of less than 1°C (at 20 mg/ml).³⁷ In addition to the low mass Type I AFP, the winter flounder has a larger (17 kDa) isoform with an extraordinarily high TH activity of 1.1°C at 0.1 mg/ml, a value not observed in any other known fish AFP.³⁸ This larger isoform helps explain how this fish survives temperatures down to –1.9°C. Nevertheless, both Type I AFP isoforms possess a “flat” ice-binding domain containing regularly spaced Thr/Asp and Thr/Asn with the Thr hydroxyl group spacing matching that of water, 16.5 Å to 16.7 Å, respectively.²⁸

Type II AFPs are the largest of the non-glycoprotein fish AFPs. Sizes range from 14 to 24 kDa and are produced by a variety of fish including smelts (*Hypomesus nipponensis* and *Osmerus mordax*), the sea raven (*Hemitrypterus americanus*) and atlantic herring (*Clupea harengus*).³⁹ These proteins have low TH values compared to other fish AFPs, achieving maximal values of only 0.78°C at 14 mg/ml.⁴⁰ Their structures are relatively complex; they are generally globular, cysteine/alanine rich, contain loop regions, α -helices and β -strands, all connected by irregular stretches of secondary structures.⁴¹ These AFPs have hydrophilic ice-binding residues Thr, Asn and Gln and can be divided into calcium-dependent (smelt and

herring) and independent (sea raven) forms. Substitutions with other divalent metal ions have shown to reduce antifreeze activity and changes to ice crystal morphology in calcium-dependent forms.⁴⁰

Type III AFPs are considered “medium” in size (~7 kDa) and globular in shape, with maximum TH of 1.4°C at 20 mg/ml and highly conserved in structure, with approximately 45% identical amino acid residues in known sequences.⁴² These AFPs can be found in high quantities in ocean pout, *Macrozoarces americanus* and Atlantic wolffish, *Anarhichas lupus* during the winter months.⁴³ Adsorption to ice is aided by the side chains containing Glu9, Asn14, Thr15/18 and Glu44 which form a flat and amphipathic ice-associating motif.⁴⁴

Lastly, Type IV is a recently discovered, 12.2 kDa lipoprotein-like AFP from the longhorn sculpin, *Myoxocephalus octodecimspinosus*. TH determinations were reported at 0.5°C at 24 mg/ml. Levels of type IV AFPs in fish are almost undetectable and are thought to have been replaced by type I AFP as Type IV is believed to lack sufficient solubility in order to provide adequate antifreeze protection, even if overexpressed.⁴⁵

Hyperactive Insect AFPs

Hyperactive AFPs are found in certain cold-adapted insects, possibly because terrestrial climates can be more challenging than ocean temperatures.⁴⁶ Two of the best-characterized and studied insect AFPs are from the spruce budworm, *Choristoneura fumiferana* (Cf) and yellow mealworm, *Tenebrio molitor* (Tm) proteins. The production of these proteins increases dramatically when the larvae overwinter, where they can experience temperatures down to minus 30°C.^{46,47} The shapes and properties of these two proteins are relatively similar. Structurally, the 9 kDa CfAFP is a left-handed β -helix with a cross-section shaped like a triangular prism and a

very flat ice-binding face, while the 8.5 kDa TmAFP is a right-handed β -helix with a cross-section fashioned more like a flattened cylinder, also having a flat ice-binding face.⁴⁸ Both these AFPs have a common Thr-X-Thr (abbreviated as TXT, where X is any amino acid), which is revealed by *in-vitro* mutagenesis to be essential in ice binding. Additionally, the hydroxyl groups in the Thr residues are similarly spaced to the oxygens in the prism plane of ice, potentially allowing for strong hydrogen bonding between the two or complementation of fit with the ice surface.⁴⁸ TH values of both these protein are amongst the highest recorded- with TmAFP producing over 3.5°C of TH at ~1 mg/ml and sbwAFP achieving greater than 5°C TH at the same concentration.⁴⁰

Plant AFPs

Apart from thermal hysteretic properties, APFs also possess the ability to inhibit ice-recrystallization (IRI), a thermodynamically-favorable process in which large ice crystals grow at the expense of small ones due to minimal ice interfacial surface area between them.⁴⁹ To date, the APF from the winter ryegrass *Lolium perenne* (LpAFP), stands out in terms of its IRI activity.⁵⁰ The 13.5 kDa LpAFP is somewhat similar in structure to insect AFPs, with repetitive sequences and high β -sheet content, forming a roll. The ice-binding site contains many Thr residues (11 of 32), as well as Ser and Val. It has been suggested that because Ser and Val have seemingly “replaced” so many Thr residues, the TH values of LpAFP are a low ~0.5°C.⁵¹ The enhanced IRI of LpAFP may occur as a result of two ice-binding sites on opposing ends of the β -roll allowing the protein to act interfacially between two growing ice crystals.⁵¹ Recent evidence, however, suggests that one ice-binding side, termed “side-a”, binds directly to ice.⁵²

B. AFP Activities

While hyperactive AFPs are 10 to 100 times more active than most fish AFPs, there is currently no unified explanation for these observations.⁴⁰ It was originally thought that the hyperactive proteins might have a better binding affinity towards ice than their weaker counterparts, but findings indicated that the difference in protein adsorption into a growing crystal from its melt were comparatively similar, at least well within an order of magnitude.⁵³ To help explain the differences in activity, more recent attention has been placed on ice-crystal morphology.

In an experiment by Scooter *et al.* (2006), ice crystals were observed to burst, or grow explosively at temperatures below the TH gap, in different configurations depending on the activity of the AFP-containing solution in which the crystals were grown. Hyperactive AFPs (irrespective of concentration or source) thwarted the growth of ice at the basal planes and caused ice crystals to burst normal to the *c*-axis, generally producing a flat hexagonal-plate crystal. In contrast, all moderately active AFPs did not show binding to basal planes and caused a burst that was parallel to the *c*-axis, with bipyramidally-shaped crystals. These observations indicated that TH represents the amount of supercooling needed to nucleate ice growth from the weakest point on the tip of the ice crystal, with this tip being more prone to growth at moderate supercooling.⁵⁴ It was concluded that hyperactive AFPs protect this region more effectively than moderate or weak AFPs.

C. Applications of AFPs

Proposed practical uses of AFPs include the cryopreservation of tissues, organs or other materials that may be of biomedical interest. There have been some promising results using

APFs in fish embryos, including turbot and seabream, as well as in media containing bull sperm, allowing these cells to become more cold-tolerant by stabilizing cell membranes and protecting cellular structures.⁵⁵⁻⁵⁷ The food industry has also shown interest in APFs for the treatment of freeze damage in meats such as beef and lamb as well as to improve taste and texture in dairy products like ice cream.⁵⁸⁻⁶⁰ Moreover, many agriculturally important crops such as wheat are threatened by frost damage, leading to large reductions in yields.⁶¹ APFs have been shown to significantly protect wheat against sub-zero temperatures as low as -7°C .⁶² Lastly, as aforementioned, two APFs, winter flounder AFP (wfAFP) and CfAFP have been proposed as novel hydrate inhibitors.³⁰ Zeng and colleagues (2006) discovered that at on a molar basis, when compared to PVP, wfAPF and CfAFP decreased induction times of THF hydrate by 4-fold and 6-fold, and decreased propane hydrate formation rate by 3-fold and 2-fold, respectively. Additionally, the proteins displayed the ability to eliminate the memory effect, something never before documented.³⁰

3. Cold-Adapted & Freeze-Thaw Tolerant Bacteria

Some bacteria have evolved to survive in cold environments and withstand the stresses of freeze-thaw by using a variety of cryoprotectants to prevent potentially deadly damage during long periods of freezing. Low-molecular mass cryoprotectants such as glucose, glycine, betaine, choline and proline as well as modifications in membrane fluidity as a result of increased carotenoids and fluidizing fatty acids are commonly utilized to inhibit cell membrane rupture.⁶³ Other, more complex molecules like the ice-nucleating proteins (INPs) are commonly produced by certain ice-nucleating bacteria, belonging to genera such as *Pseudomonas*, *Fusarium*, *Xanthomonas* and *Pantoea*.⁶⁴ The production of INPs are believed to have evolved for inciting

frost injury in plants and appeared to have been horizontally transferred to different bacterial epiphytes.⁶⁵ INPs have found utility as nucleating agents for the artificial production of snow and clouds.⁶⁶ Conversely, anti-nucleating proteins (ANPs), such as one with a mass of 55 kDa found in *Acinetobacter calcoaceticus* are able to inhibit the formation of ice nuclei, and have been found to prevent the development of ice when nucleators such as AgI, metaldehyde and ice-nucleating bacteria like *E. uredovora* are present in solution.⁶⁷

A. Bacterial AFPs

AFP_s are also found in many microorganisms. In bacteria they can act as both anti-nucleators and inhibitors of ice-growth, presumably promoting survival in permanently or seasonally frozen habitats.⁶⁸ Some examples of bacteria with antifreeze activities include *Halomonas sp.*, *Sphingomonas sp.*, *Pseudoalteromonas sp.*, and *Psychrobacter sp.* Similarly to ice crystals grown in solution with pure AFP, AFP-expressing bacteria modify ice crystal shapes to form multi-faceted or bipyramidal configurations, which closely resemble the ice structuring observed with fish AFP_s.^{69,40} Most bacteria with antifreeze capacity have been shown to possess low TH (0.1°C), and since freezing is often unavoidable, they likely use the AFP_s to control the size of ice-crystals, functioning similarly to the plant AFP_s, with low TH but effective IRI.⁷⁰

Some notable AFP-producing species include *Pseudomonas putida* GR12-2, an Arctic rhizobacterium that produces a unique 164 kDa glycolipoprotein (TH of 0.1°C) which is excreted extracellularly when the bacteria is exposed to low temperatures ($\leq 5^{\circ}\text{C}$) allowing for freeze resistance, and has the unique characteristic of possessing both antifreeze and ice-nucleating capabilities.⁷¹ Additionally, a hyperactive bacterial AFP was found in *Marinomonas*

primoryensis isolated from Antarctic lakes.⁷² This bacteria produces a large (>1 MDa), calcium-dependent protein that has two distinctive features: firstly, it is found intracellularly, unlike most other bacterial AFPs which are exported to the outside, and secondly, it has the ability to lower the freezing point of water by 2°C, making it the most active bacterial AFP known to date.⁷²

Together, the aforementioned arsenal for cold-acclimatization provides some mechanisms to withstand severe low temperature stresses. For example, freeze-thaw stress is particularly damaging, where during freezing, ice forms extracellularly, causing solutes to build up, resulting in cell dehydration and consequent membrane and protein damage.⁷³ The soil surface on the continental sides of North American mountain ranges can experience fluctuations of temperature that vary from -20°C to 20°C during the winter season as a result of Chinook winds. Subsequently, soil samples isolated from the Chinook zone (northwest Calgary) subjected to multiple freeze-thaw cycles yielded various resistant strains such as *Carnobacterium* sp., *Buttiauxella* sp., *Acinetobacter* sp., and *Chryseobacterium* sp.⁷³

B. Biotechnological Applications

Enzymes derived from psychrophiles have potential uses in a host of practical applications including detergent additives, for fabric production in the textile industry and in the food industry for various processes like juice extraction and meat tenderization.⁷⁴ As bioremediators, psychrophilic anaerobic bacteria have been implemented as treatment methods for wastewater discharge at moderate to low temperatures.⁷⁵ Moreover, as oil exploration moves further north, the likelihood of oil spills increases, as a result new research has been focused on using hydrocarbon-degrading psychrophiles isolated from soil and sea as environmentally-safe cleanup systems of oil-based pollutants in regions such as the Arctic.^{76,77}

4. Research Objectives

The purpose of this research project was to provide further understanding on the effects of both AFPs and cold-adapted, ice-associating bacteria on hydrate crystal structure and growth inhibition. The proteins selected included two AFPs, one with moderate TH levels from fish (*Zoarces americanus*) termed Type III AFP-GFP (32 kDa) and another with low TH levels from the *Lolium perenne* plant, termed LpAFP-GFP (45 kDa). Both of these recombinant proteins were tagged with green fluorescent protein (GFP, 25 kDa) which was used as a control and allowed for fluorescence under UV light. All proteins appeared stable in THF/water solutions and showed simplicity in their expression and production. Additionally, native, non-GFP tagged Type III AFP was used in a number of experiments. Preliminary studies using the GFP-tagged AFPs with sI methane hydrate were performed as well as studies on their adsorption to amorphous silica and quartz, both these studies were not included in the main body of the thesis. The major focus of the thesis was on sII hydrates, thus, two types of sII forming hydrates were tested; the model THF hydrate and a natural high-pressure propane/butane/methane (mixed gas) hydrate. The study of bacteria/protein and hydrate interactions such as adsorption and the effects on crystal growth and structure were performed using THF hydrate, since, as indicated, high-pressures are not required for its formation. Effects of proteins or bacteria on gas hydrate growth rate necessitated the use of a high-pressure gas mixture to more realistically reproduce natural hydrate formation in the field. The overriding goal of my research is to test the utility of these proteins and bacteria as novel hydrate inhibitors. It is my hope that this research may provide new insights for the development of alternative and environmentally-safe biologically-based hydrate inhibitors for use in the oil and gas industry.

References

1. Jeffrey, A. G. (1984) Hydrate Inclusion Compounds. *Journal of Inclusion Phenomena* **1**, 211-222.
2. Davy, H. (1811). The Bakerian Lecture. On Some of the Combinations of Oxymuriatic Gas and Oxygene, and on the Chemical Relations of these Principles to Inflammable Bodies. *Philosophical Transactions of the Royal Society of London* **101**, 1-35.
3. Englezos, P. (1993) Clathrate Hydrates. *Industrial and Engineering Chemistry Research* **32**, 1251-1274.
4. Berez, E. and Balla-Achs, M. (1983) Gas Hydrates, Studies in Inorganic Chemistry 4. New York, NY. Elsevier Science Publishing Co., Inc.
5. Koh, A. C. (2002) Towards a fundamental understanding of natural gas hydrates. *The Chemical Society Reviews* **31**, 157-167.
6. Larsen, R., Knight, A. C., Sloan, D. E. (1998) Clathrate hydrate growth and inhibition. *Fluid Phase Equilibria*, **150**, 353-360.
7. Bishnoi, R. P., Natarajan, V. (1996) Formation and decomposition of gas hydrates. *Fluid Phase Equilibria* **117**, 168-177.
8. Lee, S. and Holder, D. G. (2001) Methane hydrates potential as a future energy source. *Fuel Processing Technology* **71**, 181-186.
9. Sloan D. E. (2003) Fundamental principles and applications of natural gas hydrates. *Nature* **426**, 353-363.
10. Jo, D. Y. and Ahn, J. B. (2002) Analysis of hazard areas associated with high-pressure natural-gas pipelines. *Journal of Loss Prevention in the Process Industries* **15**, 179-188.
11. Gbaruko, C. B., Igwe, C. J., Gbaruko, N. P. and Nwokeoma, C. R. (2007) Gas hydrates and clathrates: Flow assurance, environmental and economic perspectives and the Nigerian liquefied natural gas project. *Journal of Petroleum Science and Engineering* **56**, 192-198.
12. Sun, Z., Ma, R., Fan, S., Guo, K. and Wang, R. (2004) Investigations on Gas Storage in Methane Hydrate. *Journal of Natural Gas Chemistry* **13**, 107-112.
13. Gudmundsson, S. J. and Borrehaug, A. (1996) Frozen hydrate for transportation of natural gas. Second International Conference on Natural Gas Hydrate, Toulouse, France, 2-6 June 1996, pp. 415-422.
14. Hao, W., Wang, J., Fan, S. and Hao, W. (2008) Evaluation and analysis method for natural gas hydrate storage and transportation processes. *Energy Conversion and Management* **49**, 2546-2553.

15. Davies, R. S., Selim, S. M., Sloan, D. E., Bollavaram, P. and Peters, J. D. (2006) Hydrate Plug Dissociation. *American Institute of Chemical Engineers Journal* **52**, 4016.
16. Hammerschmidt, E. G. (1943) Formation of gas hydrates in natural gas transmission lines. *Industrial and Engineering Chemistry Research* **26**, 851.
17. Peytavy, J. L., Gleantm, P. and Bourgm, P. (2008) Qualification of Low Dosage Hydrate Inhibitors (LDHIs): Field Cases Studies Demonstrate the Good Reproducibility of the Results Obtained from Flow Loops. Proceedings of the 6th International Conference on Gas Hydrates (ICGH 2008) Vancouver, British Colombia, Canada, July 6-10, 2008.
18. Elieff, M. A. B. (2006) Top hole drilling with dual gradient technology to control shallow hazards. Master's thesis, Texas A&M University, College Station, Texas, USA.
19. Sloan, D. E. and Koh, A. C. (2007) Clathrate Hydrates of Natural Gases, 3rd Ed. Fl: CRC Press.
20. Rubeiro, C. and Lage, C. L. P. (2008) Modelling of hydrate formation kinetics: State-of the-art and future directions. *Chemical Engineering Sciences* **63**, 2007-2034.
21. Natarajan, V., Bishnoi, R. P. and Kalogerakis, N. (1994) Induction phenomena in gas hydrate nucleation. *Chemical Engineering Science* **49**, 2075–2087.
22. Buchanan, P., Soper, K. A., Thompson, H. and Westacott, E. R. (2005) Search for memory effects in methane hydrate: Structure of water before hydrate formation and after hydrate decomposition. *Journal of Chemical Physics* **123**, 164507.
23. Rodger, P. M. (1990) Stability of Gas Hydrates. *Journal of Physical Chemistry* **94**, 6080-6089.
24. Koh, A. C., Westacott, E. R., Zhang, W., Hirachand, K., Creek, L. J. and Soper, K. A. (2002) Mechanisms of gas hydrate formation and inhibition. *Fluid Phase Equilibria* **30**, 143-151.
25. Clark, L. W., Anderson, J., Barr, N. and Kremer, E. 2008. GUAP3 Scale Dissolver and Scale Squeeze Application Using Kinetic Hydrate Inhibitor (KHI). Proceedings of the 6th International Conference on Gas Hydrates (ICGH 2008), Vancouver, British Columbia, Canada, July 6-10, 2008.
26. Lederhos, P. L., Long, P. J., Sum, A., Christiansen, L. R. and Sloan Jr., D. E. (1996) Effective kinetic inhibitors for natural gas hydrates. *Chemical Engineering Science* **51**, 1221-1229.
27. Makogon, Y. T. and Sloan, D. E. (2002) Mechanisms of Kinetic Hydrate Inhibitors, Proc 4th International Hydrate Conference, Yokohama, Japan.
28. Barret, J. (2001) Thermal hysteresis proteins. *The International Journal of Biochemistry & Cell Biology*, **33**, 105-117.

29. Huo, Z., Freer, E., Lamar, M., Sannigrahi, B., Knauss, M. D. and Sloan Jr., D. E. (2001). Hydrate plug prevention by anti-agglomeration. *Chemical Engineering Science* **56**, 4979-4991.
30. Zeng, H., Wilson, D. L., Walker, K. V. and Ripmeester, A. J. (2006) Effect of Antifreeze Proteins on the Nucleation, Growth, and the Memory Effect during Tetrahydrofuran Clathrate Hydrate Formation. *Journal of American Chemical Society* **128**, 2844-2850.
31. Kristiansen, E. and Zachariassen, E. K. (2005) The mechanism by which fish antifreeze proteins cause thermal hysteresis, *Cryobiology* **51**, 262-280.
32. Scholander, F. P., Gordon, M. S. and Ben, H. Freezing Resistance in Some Northern Fishes. *Amdur Biological Bulletin* **122**, 52-62.
33. DeVries, L. A. and Wohlschlag, D. E. (1969) Freezing Resistance in Some Antarctic Fishes. *Science* **7**, 1073-1075.
34. Harding, M. M., Andergerg, I. P. and Haymet, J. D. A. (2003) Antifreeze glycoproteins from polar fish. *European Journal of Biochemistry* **270**, 1381-1392.
35. Knight, A. C., Driggers, E. and DeVries L. A. (1993) Adsorption to ice of fish antifreeze glycoproteins 7 and 8. *Biophysics Journal* **64**, 252-259.
36. Ewart, V. K. (2002) Fish Antifreeze Proteins, Singapore: World Scientific Publishing Co., Pte., Ltd.
37. Chapsky, L. and Rubinsky, B. (1997) Kinetics of antifreeze protein-induced ice growth inhibition, *Federation of the Societies of Biochemistry and Molecular Biology Letters* **412**, 241-244.
38. Marshall, B. C., Fletcher, L. G. and Davies, L. P. (2004) Hyperactive antifreeze protein in a fish. *Nature* **429**, 153.
39. Liu, Y., Li, Z., Lin, Q., Kosinski, J., Seetherman, J., Bujnicki, M. J., Sivaraman, J. and Hew, C. (2007) Structure and Evolutionary Origin of Ca²⁺-Dependent Herring Type II Antifreeze Protein. *Public Library of Science* **2**, e548.
40. Scotter, J. A., Kuntz, A. D., Saul, M., Graham, A. L., Davies, L. P. and Rose, R. D. (2006) Expression and purification of sea raven type II antifreeze protein from *Drosophila melanogaster* S2 cells. *Protein Expression and Purification* **47**, 374-383.
41. Nishimiya, Y., Kondo, H., Takamichi, M., Sugimoto, H., Suzuki, M., Miura, A. and Tsuda, S. (2008) Crystal Structure and Mutational Analysis of Ca²⁺-Independent Type II Antifreeze Proteins from Longsnout Poacher, *Brachyopsis rostratus*. *Journal of Molecular Biology* **328**, 734-746.

42. Antson, A. A., Smith, J. D., Roper, I. D., Lewis, S., Caves, D.S. L., Verma, S.C., Buckley, L. S., Lillford, J. P., Hubbard, E. R. (2001) Understanding the mechanism of ice binding by type III antifreeze proteins. *Journal of Molecular Biology* **305**, 875-889.
43. Chao, H., Davies, L. P., Sykes, D. B. and Sonnichsen, D. F. (1993) Use of proline mutants to help solve the NMR solution structure of type III antifreeze protein. *Protein Science* **2**, 1411-1428.
44. Graether, P. S., DeLuca, I. C., Baardsnes, J., Hill, A. G. and Davies, L. P. (1999) Quantitative and Qualitative Analysis of Type III Antifreeze Protein Structure and Function. *Journal of Biological Chemistry* **274**, 11842-11847.
45. Gauthier, Y. S., Scotter, J. A., Lin, F., Baardsnes, J., Fletcher, L. G. and Davies, L. P. (2008) A re-evaluation of the role of type IV antifreeze protein. *Cryobiology* **57**, 292-296.
46. Tyshenko, G. M., Doucet, D., Davies, L. P. and Walker, K. V. (1997) The antifreeze potential of the spruce budworm thermal hysteresis protein. *Nature* **15**, 887-890.
47. Qin, W. and Walker, V.K. (2006) *Tenebrio* antifreeze protein gene identification and regulation. *Gene* **367**, 142-149.
48. Graether, P. S. and Sykes, D. B. (2004) Cold survival in freeze-intolerant insects: the structure and function of the β -helical antifreeze proteins. *European Journal of Biochemistry*. **271**, 3285-3296.
49. Tomczak, M. M., Marshall, B. C., Gilbert, A. J and Davies, L. P. (2003) A facile method for determining ice recrystallization inhibition by antifreeze proteins. *Biochemical and Biomedical Research Communications* **311**, 1041-1046.
50. Sidebottom, C., Buckley, S., Pudney, P., Twigg, S., Jarman, C., Holt, C., Telford, J., McArthur, A., Worrall, D., Hubbard, R. and Lillford, P. (2000) Phytochemistry: Heat-stable antifreeze protein from grass. *Nature* **406**, 256.
51. Kuiper, J. M., Davies, L. P. and Walker, K. V. (2001) A Theoretical Model of a Plant Antifreeze Protein from *Lolium perenne*. *Biophysical Journal* **81**, 3560-3565.
52. Middleton, J. A., Brown, M. A., Davies, L. P. and Walker, K. V. (2009) Identification of the ice-binding face of a plant antifreeze protein. *Federation of the Societies of Biochemistry and Molecular Biology Letters* **583**, 815-819.
53. Marshall, C. B., Tomczak, M. M., Gauthier, Y. S., Kuiper, J. M., Lankin, C., Walker, K. V. and Davies, L. P. (2004) Partitioning of fish and insect antifreeze proteins into ice suggests they bind with comparable affinity. *Biochemistry* **43**, 148-154.
54. Scotter, J. A., Marshall, C. B., Graham, A. L., Gilbert, A. J., Garnham, P. C. and Davies, L. P. (2006) The basis for hyperactivity of antifreeze proteins. *Cryobiology* **53**, 229-239.

55. Robles, V., Cabrita, E., Anel, L. and Herráez, P. M. (2006) Microinjection of the antifreeze protein type III (AFPIII) in turbot (*Scophthalmus maximus*) embryos: Toxicity and protein distribution. *Aquaculture* **4**, 1299-1306.
56. Robles, V., Barbosa, V., Herráez, P. M., Martínez-Páramo, S. and Cancela, L. M. (2007) The antifreeze protein type I (AFP I) increases seabream (*Sparus aurata*) embryos tolerance to low temperatures. *Theriogenology* **68**, 284-289.
57. Prathalingam, S. M., Holt, V. W., Revell, G. S., Mirczuk, S., Fleck, R. A. and Watson, F. (2006) Impact of antifreeze proteins and antifreeze glycoproteins on bovine sperm during freeze-thaw. *Theriogenology* **66**, 1894-1900.
58. Payne, R. S., Sandford, D., Harris, A. and Young, A. O. (1994) The effects of antifreeze proteins on chilled and frozen meat. *Meat Science* **37**, 429-438.
59. Payne, R. S., and Young, A. O. (1995). Effect of pre-slaughter administration of antifreeze proteins on frozen meat quality. *Meat Science* **41**, 147-155.
60. Warren, C. J., Mueller, C. M. and Mckown, R. L. (1992). Ice crystal growth suppression polypeptides and methods of preparation. US Patent 5,118,792.
61. Aggarwal, K. P., Kalra, N., Chander, S., Pathak, H. (2006) InfoCrop: A dynamic simulation model for the assessment of crop yields, losses due to pests, and environmental impact of agro-ecosystems in tropical environments. I. Model description. *Agricultural Systems* **89**, 1-25.
62. Khanna, H. K. and Daggard, G. E. Targeted expression of redesigned and codon optimised synthetic gene leads to recrystallisation inhibition and reduced electrolyte leakage in spring wheat at sub-zero temperatures (2006) *Plant Cell Reports* **25**, 1336-1346.
63. Chattopadhyay K M (2002) Bacterial Cryoprotectants, *Resonance* **7**, 59-63.
64. Gurian-Sherman, D. and Lindow, E. S. (1993) Bacterial ice nucleation: significance and molecular basis. *Federation of American Societies for Experimental Biology Journal* **7**, 1338-1343.
65. Junge, K. and Swanson, D. B. (2008) High-resolution ice nucleation spectra of sea-ice bacteria: Implications for cloud formation and life in frozen environments. *Biogeosciences* **5**, 865-873.
66. Christner, B. C., Morris, C. E., Foreman, C. M., Cai, R. and Sands, D. C. (2008). Ubiquity of biological ice nucleators in snowfall. *Science* **319**, 1214.
67. Kawahara, H. (2002) The Structures and Functions of Ice Crystal-Controlling Proteins from Bacteria, *Journal of Bioscience and Bioengineering* **94**, 492-496.

68. Xu, H., Griffith, M., Patten, L. C., and Glick R. B. (1998). Isolation and characterization of an antifreeze protein with ice nucleation activity from the plant growth promoting rhizobacterium *Pseudomonas putida* GR12-2. *Canadian Journal of Microbiology* **44**, 64-73.
69. Kawahara, H. (2008) Psychrophiles: from Biodiversity to Biotechnology, Germany: Springer-Verlag Berlin Heidelberg.
70. Kawahara, H., Nakano, Y., Omiya, K., Muryoi, N., Nishikawa, J. and Obata, H. (2004) Production of two types of ice crystal-controlling proteins in Antarctic bacterium, *Journal of Bioscience and Bioengineering* **98**, 220-223.
71. Muryoi, N., Sato, M., Kaneko, S., Kawahara, H., Obata, H., Yaish, F. W. M., Griffith, M. and Glick, R. B. (2004) Cloning and Expression of *afpA*, a Gene Encoding an Antifreeze Protein from the Arctic Plant Growth-Promoting Rhizobacterium *Pseudomonas putida* GR12-2. *Journal of Bacteriology* **186**, 5661-5671.
72. Gilbert, A. J., Davies, L. P. and Laybourn-Parry, J. (2005) A hyperactive, Ca²⁺-dependent antifreeze protein in an Antarctic bacterium, *FEMS Microb. Lett.* **245**, 67-72.
73. Walker, K. V., Palmer, R. G. and Voordouw, G. (2005) Freeze-Thaw Tolerance and Clues to the Winter Survival of a Soil Community. *Applied and Environmental Microbiology* **72**, 1784-1792.
74. Gerday, C., Aittaleb, M., Bentahir, M., Chessa, J., Claverie, P., Collins, T., D'Amico, S., Dumont, J., Garsoux, G., Georgette, D., Hoyoux, A., Lonhienne, T., Meuwis and M., Feller, G. (2000) Cold-adapted enzymes: from fundamentals to biotechnology, *Trends in Biotechnology* **18**, 103-107.
75. Lettinga, G., Rebac, S. and Zeeman, G. (2001) Challenge of psychrophilic anaerobic wastewater treatment, *Trends in Biotechnology* **19**, 363-370.
76. Brakstad, G. O., Nonstad, I., Faksness, L., Brandvik, J. P. (2007) Responses of Microbial Communities in Arctic Sea Ice After Contamination by Crude Petroleum Oil, *Microbial Ecology* **55**, 540-552.
77. Okoh, I. A. (2006) Biodegradation alternative in the cleanup of petroleum hydrocarbon pollutants, *Biotechnology and Molecular Biology Review* **1**, 38-55.
78. Hester C K, Gupta A, Rovetto J L, Ohno H, Wierzchowski S, Boxall J, Davies S, Nicholas J, Rensing P, Strobel T, Greaves D, Lachance J, Walsh M, Dieker L, Timm C, Green G, Hughson A, Papineau A, Sikora B, Dec F S, Miller T K, Sloan D E, Koh A C (2007) Gas Hydrates in Energy Recovery, Transportation and Storage. Energy Seminar, Stanford University, April 18, 2007. Obtained Online at: <http://deimos3.apple.com/WebObjects/Core.woa/FeedEnclosure/itunes.stanford.edu.1299566665.01299566668.1314567602/enclosure.pdf>

79. Anderson B (2005) Molecular Modeling of Hydrate-Clathrates via ab initio, Cell Potential, and Dynamic Methods. Thesis (Ph.D), Massachusetts institute of Technology, Dept. of Chemical Engineering.

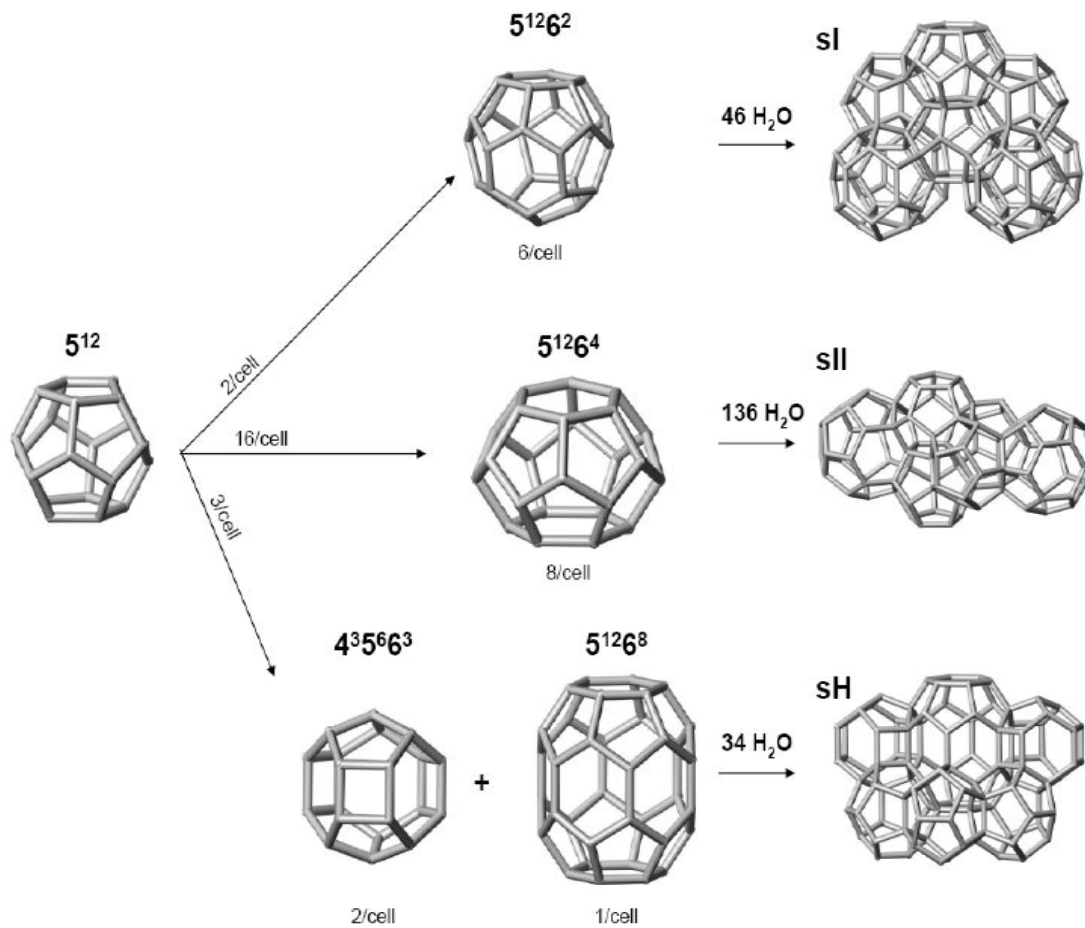


Figure 1.1. The three most commonly observed clathrate hydrate structures: sI, sII and sH. The diagram outlines the structure and quantity of different cages that compose the unit cell of each hydrate. For example, sII is composed of 16 pentagonal dodecahedral cavities (denoted as 5^{12}) and 8 hexacaidecahedral cavities (denoted as $5^{12}6^4$) that forms a unit cell of 136 water molecules.⁷⁸

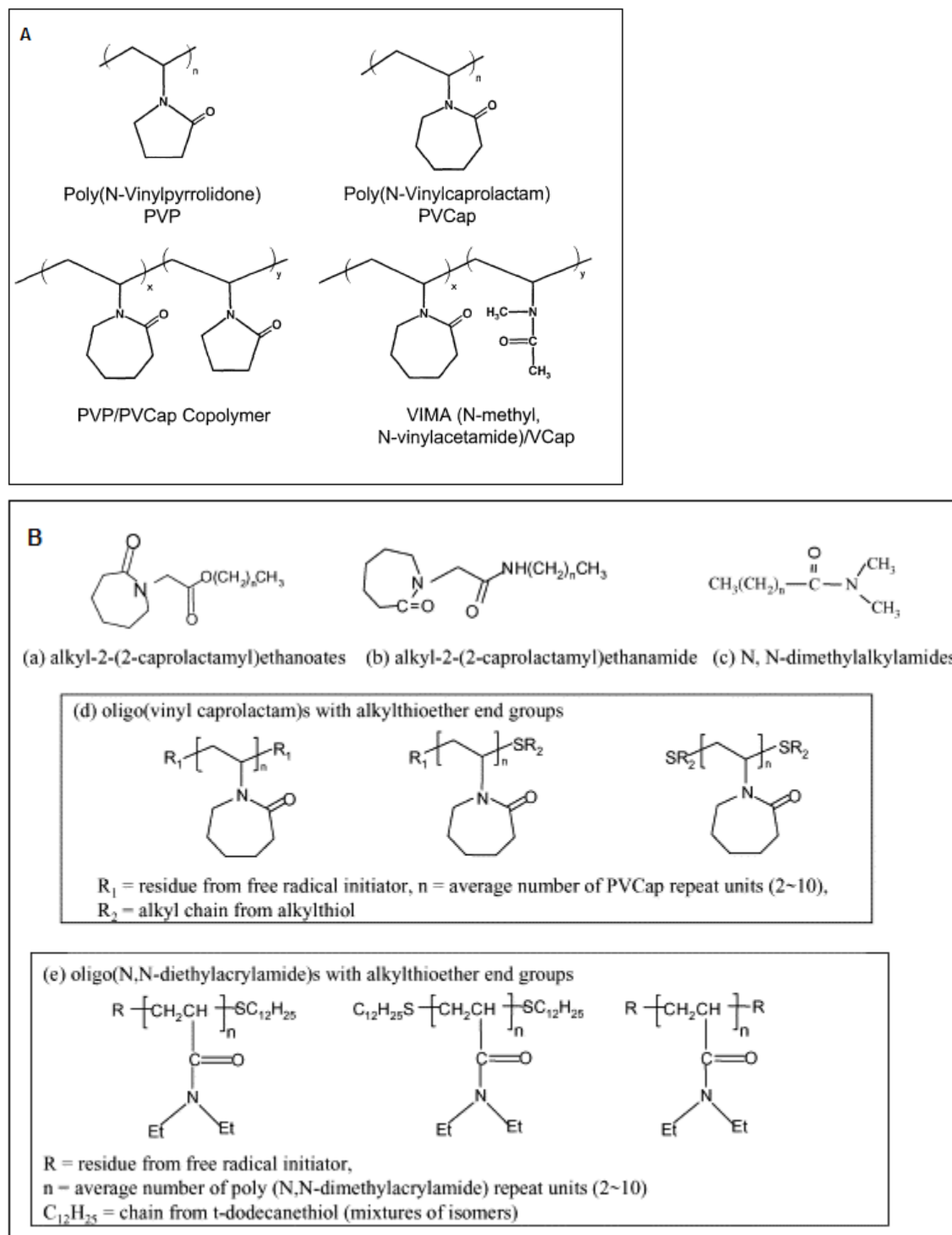


Figure 1.2. Low Dosage Hydrate Inhibitors. (A) Examples of some common kinetic hydrate inhibitors.⁷⁹ (B) Examples of some common antiagglomerants.⁷⁹

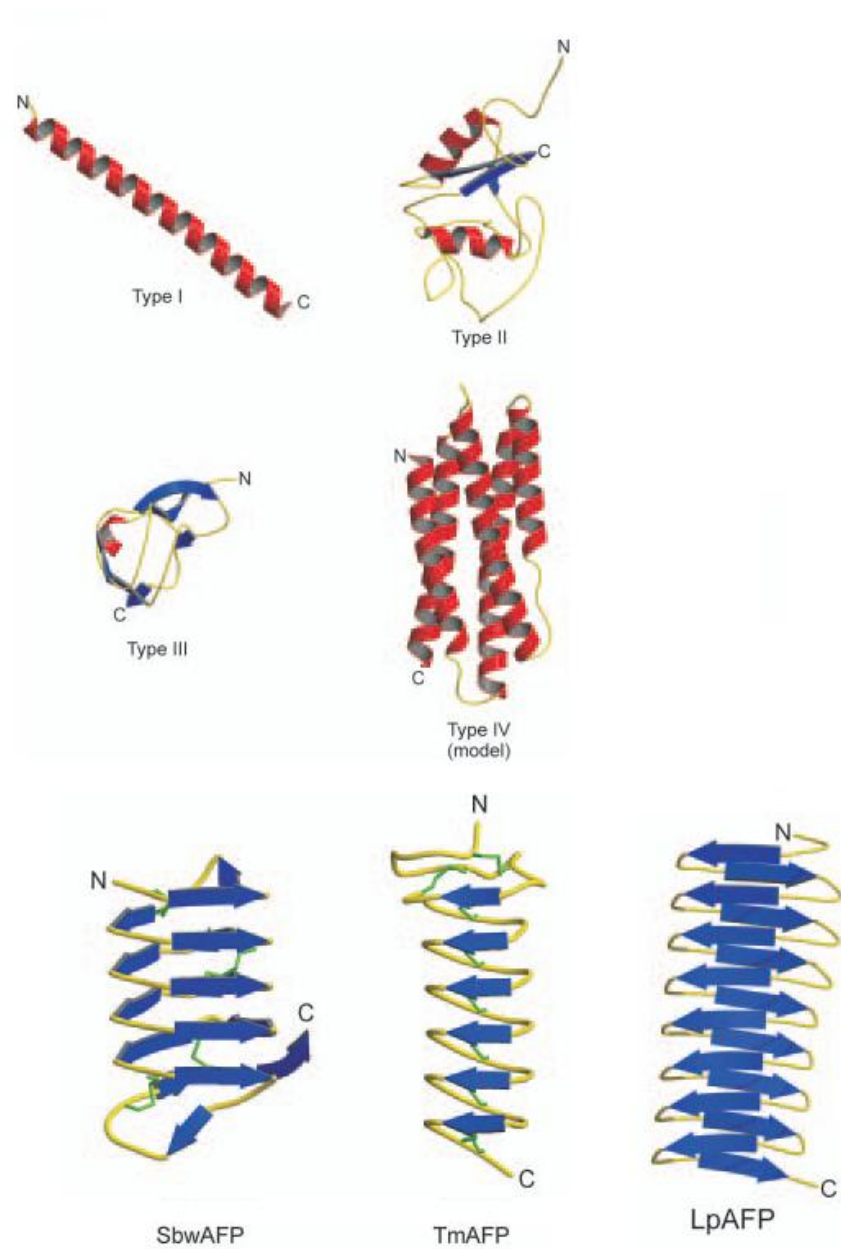


Figure 1.3. Ribbon diagrams of determined and predicted structural models of fish (top four), insect (bottom left and center) and plant AFPs (bottom left). α -helices are represented as red and β -strands as blue, disulphide bonds are shown as green sticks in the TmAFP and SbWAFP .⁴⁸

Chapter 2

Towards a Green Hydrate Inhibitor: Imaging Antifreeze Proteins on Clathrates

Raimond Gordienko*, Hiroshi Ohno†, Vinay K. Singh‡, Zhongchao Jia‡, John. A. Ripmeester† and Virginia K. Walker*.

Departments of Biology* and Biochemistry‡, Queen's University, Kingston ON, K7L 3N6, Canada. Materials Structure and Function Group†, National Research Council Canada, Ottawa ON, K1A 0R6, Canada.

Abstract

The formation of hydrate plugs in oil and gas pipelines is a serious industrial problem. There has been an increased interest in the use of alternative hydrate inhibitors as substitutes for thermodynamic inhibitors like methanol. It was been shown that antifreeze proteins (AFPs) posses the ability to modify structure II (sII) tetrahydrofuran (THF) hydrate crystal morphologies by adhering to the hydrate surface and inhibiting growth in a similar fashion to the kinetic inhibitor poly-N-vinylpyrrolidone (PVP). The effects of AFPs on the formation and growth rate of high-pressure sII gas mix hydrate were also tested and proved AFPs possessed superior hydrate inhibition to PVP. The results indicated that AFPs may be a suitable model for studying new inhibitor systems and is a step towards the development of biologically-based hydrate inhibitors.

Introduction

Gas hydrates, or clathrates, are ice-like compounds that form when hydrocarbon-based guest molecules are trapped in hydrogen-bonded water cages that form under high pressures and low temperatures.¹ Natural gas hydrates most commonly exist as one of two structures. Small guest molecules such as methane tend to form structure I (sI) hydrates while larger guests like propane form structure II (sII) hydrates.² In the laboratory, gas hydrates are conventionally modeled using tetrahydrofuran (THF) which is enclathrated at atmospheric pressures.³ THF hydrate forms cubic sII clathrates, similar to the hydrates that form in pipelines during oil and gas production.⁴

Recently, the petroleum industry has been moving into deeper waters which present prime conditions for hydrate growth. Hydrate plugs impede oil and gas flow, resulting in equipment damage as well as hazardous working conditions that can even result in blowouts.⁵ Thermodynamic inhibitors such as methanol are one of the most common practical methods of controlling hydrate formation.⁶ However, as a result of the high costs, flammability and environmental toxicity associated with such inhibitors, there has been a shift towards the less toxic and sometimes cheaper alternative kinetic hydrate inhibitors, which delay nucleation and interfere with crystal growth, as well as antiagglomerants, which act to prevent hydrates from aggregating into larger masses.^{7,8}

These concerns have prompted us to investigate the potential inhibitory effects of antifreeze proteins (AFPs) on hydrates. AFPs are a diverse class of proteins that were first identified in fish during the 1950s and have since been found in cold-adapted bacteria, plants and insects.⁹⁻¹² Despite differences in structure, they have the common ability to adsorb to ice using specific ice-binding faces. AFPs lower the freezing point of water as a result of increased local

curvature of growing ice around the adsorbed protein, resulting in a difference between the freezing and melting points, a phenomenon known as thermal hysteresis (TH).¹³

We have previously proposed AFPs as alternative hydrate inhibitors models.¹⁴ Here we image fluorescently-tagged AFPs and the effects of these proteins on THF hydrate crystals. We also determined the inhibitory effects of these AFPs on the gas consumption and growth rates of sII methane/ethane/propane hydrate as part of our efforts towards the development of alternative, biologically-based hydrate inhibitors.

Materials and Methods

Bacterial Strains and THF solutions

The AFP cloned from the perennial grass, *Lolium perenne* (Lp), has a low TH while the ocean pout fish Type III AFP is more active.^{9,11} Sequences encoding these AFPs, with or without a green fluorescent protein (GFP) label, were expressed in *E. coli* BL21 cells. The plasmids used included the pET-24 vector (Novagen) for the expression of Type III AFP (7 kDa) and LpAFP-GFP (45 kDa), and pET-20b (Novagen) for Type III AFP-GFP (32 kDa). A plasmid encoding a control GFP (25 kDa) without an AFP sequence, was made by the amplification of GFP from the pET-20 vector expressing the Type III AFP-GFP sequence using primers with a 5'-NdeI site and a 3'-HindIII site. The amplified GFP was then inserted into a pET24a vector between its NdeI/HindIII sites, followed by subsequent transformation of BL21 cells. The insert was verified by sequencing. All of the recombinant proteins were tagged with a poly(His)₆ sequence located on the C-terminals of the expressed proteins to facilitate purification.

THF ($\geq 99.5\%$, Sigma-Aldrich, St. Louis, MO, USA) was mixed with distilled water or water containing solutions of proteins or other additives, at a 1:15 molar ratio or 1: 3.34 (v/v) as

previously described.³ The observed crystallization temperature was the same as published values (<4.4°C).¹⁵

Bioreactor: Production and Purification

Recombinant *E. coli* BL21 cells were grown in a New Brunswick Bio-Flow 110 bioreactor (Edison, NJ, USA) using Luria-Bertani (LB) media enriched with 5 g/L yeast extract, 6 g/L glucose, 12 g/L Na₂HPO₄, 6 g/L K₂HPO₄, 2 g/L NH₄Cl, 0.022 g/L CaCl₂ and 0.482 g/L MgSO₄ at 37°C, pH 7, 650 RPM agitation and 4 L/min air flow, until the culture reached OD₆₀₀ = 8 or the dissolved oxygen (DO) levels were at a minimum (0-20%). The culture temperature was then decreased to 20°C, and recombinant protein expression was induced with 1 mM isopropyl β-D-1-thiogalactopyranoside (IPTG) for 16 h. The cells were harvested by centrifugation (6000 × g, 4°C, for 20 min) and resuspended in cold lysis buffer (20 mM Tris, 500 mM NaCl, pH 7, containing an EDTA-free protease inhibitor cocktail (Mini pills; Roche, Mannheim, Germany)).

The pelleted cells were then lysed using a Branson sonicator for 4 min with 1 min cooling on ice and centrifuged (16,000 × g, 4°C for 40 min) to remove solid cell debris. The supernatant was then mixed with cobalt-based agarose Talon Metal Affinity Resin (BD Bioscience, Mountain View, CA, USA) and incubated for 1.5 h at 4°C with mild shaking, allowing the poly(His)-tagged proteins to bind to the resin. The supernatant/resin mixture was then loaded onto a 100 ml column and the resin was washed twice with wash buffer (20 mM Tris, 500 mM NaCl, pH 7), once with wash buffer containing 5 mM imidazole, followed by 10 mM imidazole and finally eluted with 20 mM and 250 mM imidazole. The purified protein was then visualized on a 12% SDS-PAGE gel stained with Coomassie Brilliant Blue R-250. Protein concentration was determined using dye-binding via bicinchurinic acid assay (BCA Protein

Assay Kit; Pierce, Rockford, IL, USA). Thermal hysteresis (TH) was measured as previously described,¹⁶ with a nanolitre osmometer at protein concentrations of approximately 4 mg/ml (Clifton Technical Physics, Hartford, NY, USA).

Polycrystalline THF Hydrate

Polycrystalline THF hydrate was grown on a hollow brass finger connected to a temperature-programmable 1197P water bath (VWR International, Mississauga, ON) filled with a water/ethylene glycol mixture (at 3:1 v/v). A solution of THF/water (1:3.34, v/v; 80 ml) was cooled to 4°C and poured into a 100 ml glass beaker, placed in an insulated styrofoam box. The cooled brass finger (2.5°C) was submerged into the THF/water solution, which was stirred with a magnetic stir bar. To expedite hydrate formation, a small piece of THF hydrate crystal was added into the solution, which helped nucleate a thin layer of hydrate on the surface of the brass finger, a process known as seeding. When the THF hydrate uniformly covered the finger, the beaker was removed and replaced with another containing 80 ml of the test solution, and sealed with parafilm to prevent the evaporation of THF.

Test solutions consisted of THF/water (1:3.34, v/v; 80 ml) containing 2 µM, 4 µM, 8 µM and 16 µM of purified recombinant LpAFP-GFP, Type III AFP-GFP and GFP. THF polycrystals were grown for 8 h with the ethylene/glycol bath set to an initial temperature of 0°C and a final temperature of -6.5°C, with a 0.5°C drop every 30 min. The temperature of the THF/water/protein solution surrounding the growing crystal remained at ~-4.9°C for the duration of the experiment. At the conclusion of the growth period, the beaker was removed and the adhered polycrystal was wrapped in aluminum foil and placed in ice to prevent it from melting.

The bath temperature was then increased to 5.5°C, heating the brass finger and allowing the crystal to be collected.

After washing the crystal with 30 ml of distilled water (<4°C) to remove any residual solution, it was weighed and examined under ultraviolet light (midway wavelength = 302 nm) at 4°C and photographed. After melting the polycrystals at room temperature, the solution was concentrated to 2 ml with a 15 ml concentrating tube (Millipore, Billeveica, MA, USA), and the total amount of protein was determined using the BCA assay. The amount of recombinant protein adsorbed per gram of hydrate crystal (denoted as mol/g_{crystal}) was calculated and a Tukey-Kramer test was used for statistical comparisons.

Single Crystal THF Hydrate

Single THF hydrate crystals were formed at 3°C (1.4°C supercooling) by placing a glass Pasteur pipette, held in place by a central hole punched through a rubber stopper, into a beaker sealed with parafilm containing 80 ml THF solution. Recombinant AFPs, GFP or a commercial hydrate inhibitor, poly-N-vinylpyrrolidone (PVP) (MW 10,000; Sigma-Aldrich, St. Louis, MO, USA) were added at 15, 50, 100 and 200 µg/ml to observe changes in THF single crystal morphology. To determine the effects of high supercooling rates on crystal structure, these crystals were grown at 0°C and -1.5°C. Crystal growth was initiated inside the pipette by nucleating the solution with a supercooled copper wire placed in dry ice, as described by Knight and Ryder.¹⁷ THF hydrate was formed down the pipette's decreasing diameter until a single, octahedral crystal emerged from the tip. If more than one crystal was initiated, or the beaker was jarred, the experiment was discontinued, as this resulted in polycrystalline growth. This crystal was grown slowly for approximately 6 h, or until the crystal edges touched the beaker walls.

When complete, the crystal was removed from the solution and frozen at -20°C until observations on the crystal morphology and digital photographs (Nikon, Coolpix S10) were recorded.

sII Gas Hydrate

Recombinant proteins Type III AFP-GFP, LpAFP-GFP, Type III AFP and GFP, as well as PVP were mixed at 0.1 mM concentrations with 1000 Å pore diameter silica gel (Silicycle Chemicals, St. Jean-Baptiste, QC) at a ratio of 1 to 1.3 (v/w) respectively, to allow for rapid nucleation, as described by Seo and colleagues,¹⁸ and modified by Ohno *et al* (in preparation). Briefly, the silica sand/additive mix was added into a stainless steel cell. After the sample system was immersed into a water bath set to 25°C , the sample was purged twice by a natural gas mix consisting of 2% propane, 5% ethane and 93% methane (Linde Canada, Mississauga, ON) at approximately 250 PSI (1.7×10^4 mbar), and then was pressurized to 1000 PSI (6.9×10^4 mbar) with the same gas mixture. Hydrate nucleation was initiated by transferring the pressurized cell into another water bath set to 0.5°C . Hydrate formation was monitored by a sudden drop in pressure (recorded using an Omega DAQPRO-5300; Fourier Systems, Fairfield, CT, USA). Moles of gas consumed (nGas), indicating the amount of hydrate formed, were calculated as previously described.¹⁹

$$n\text{Gas} = V_{sv} (P/zRT)_0 - V_{sv} (P/zRT)_t$$

This relationship allows to determine the difference between moles of gas at time $t = 0$ and the number of moles of gas at time t , where the V_{sv} is the volume of the gas phase, P is pressure, R is the gas constant, T is temperature and z is the compressibility factor, calculated by Pitzer's correlations.²⁰ Additionally, the rate of change of gas consumption, denoted as nGas/min

(indicative of the rate of hydrate growth), was calculated by determining the average of the slopes of all nGas data points (slope = $\Delta n\text{Gas}/\Delta\text{time}$). Both nGas and slopes were calculated up to the time-period of 1,500 min.

Results

Bioreactor yields

The bioreactor yields were comparable for the recombinant proteins, although optimization of protein production can depend on a variety of conditions including total volume of growth media, level of DO or OD₆₀₀ at IPTG induction as well as temperature during the induction period (Fig. 2.1). Although most of these parameters were kept as constant as possible, it was generally found that lower induction temperatures ($\leq 20^\circ\text{C}$), yielded the highest amounts of protein. Final purified yields for reactor volumes of 3.5 to 4 L ranged from 180 to 260 mg. Purified recombinant proteins were seen as single bands on a 12% SDS-PAGE gel (Fig. 2.2). Thermal hysteresis values for the AFPs were calculated at $0.10 \pm 8.5 \times 10^{-3}^\circ\text{C}$ for LpAFP-GFP, $0.48 \pm 2.8 \times 10^{-2}^\circ\text{C}$ for Type III AFP-GFP and $0.43 \pm 2.8 \times 10^{-2}^\circ\text{C}$ for Type III AFP, GFP showed no TH. All proteins were tested at ~ 4 mg/ml.

Recombinant GFP-labeled proteins and polycrystalline THF hydrate

Polycrystalline THF hydrate crystals grown in the presence of GFP-tagged AFPs were obviously fluorescent green under UV illumination (Fig. 2.3). Conversely when hydrate was grown in the presence of recombinant GFP alone, the hydrates were uniformly dark. In an effort to quantify the adsorption, the hydrates were melted and assayed for adsorbed protein (μmoles of recombinant protein adsorbed per gram of crystal, Fig. 2.4). For both purified LpAFP-GFP and

Type III AFP-GFP fusion proteins, there was a linear correlation between the amount of protein adsorbed into the growing THF hydrate and the concentration of the protein in the THF solution. At lower concentrations (2 and 4 μM) more Type III AFP-GFP appeared to bind than LpAFP-GFP, with an average of 44.0 % more adsorbed. At higher concentrations (8 and 16 μM) LpAFP-GFP adsorbed an average of 42.5% more than Type III AFP. All differences between the two AFP-GFPs were statistically significant. In contrast, no adsorption of GFP was detected in the crystals at any concentration, with the exception of 2 μM , where an average of 7.9×10^{-5} $\mu\text{moles/g}_{\text{crystal}}$ was detected. At all other concentrations, differences in the amounts of adsorbed GFP compared to the two AFP-GFPs were statistically significant.

AFPs and Single THF Hydrate Crystals

Since the fusion proteins adsorbed to polycrystalline THF hydrate, single THF hydrate crystals were slowly grown at low supercooling (3°C or 1.4°C below the THF solution crystallization point) to observe if the presence of the proteins could change crystal morphology. With no proteins, or in the presence of low to moderate concentrations of GFP (Fig. 2.5A), crystals exhibited a cubic octahedral shape that is characteristic of THF hydrate at these conditions.¹⁵ The {111} planes were clearly defined and there were no apparent modifications to crystal shape.

In striking contrast, when single crystals were grown under the same conditions, but in the presence of recombinant AFPs, they exhibited hopper-like or skeletal morphologies (Fig. 2.5B), characteristic of the interference of normal crystal growth habit.¹⁷ At all but the lowest concentration of LpAFP-GFP, depressions were observed on the interior {111} faces. Similar morphologies were seen in crystals grown in solutions of Type III AFP-GFP (50-200 $\mu\text{g/ml}$).

Interestingly, only the non-GFP tagged Type III AFP displayed clear skeletal shaping at the lowest concentration (15 $\mu\text{g/ml}$), but this protein was not possible to test at other concentrations, as it precipitated easily in THF solution. As indicated, recombinant GFP did not appear to alter crystal morphology until tested at high concentrations (100 and 200 $\mu\text{g/ml}$) and even then showed one to two shallow hopper depressions. When the crystals grown in AFP-GFP solutions were observed under UV light, it appeared that the protein had adsorbed uniformly throughout the entire cubic crystal and at every face (Fig. 2.5C). Consistent with the observation of morphology, there was no evidence of GFP adsorption at low to moderate concentrations.

In order to observe the effect of a known sII inhibitor on the growth habit of single THF hydrate crystals, crystals were grown in solutions containing PVP. In all but the lowest concentration of PVP, single crystals were hopper-like and similar to those grown in the presence of AFPs, the depressions on the $\{111\}$ faces becoming more pronounced as the concentration of PVP increased (Fig. 2.5D).

It should be noted that all these crystals were grown slowly at temperatures just below the THF hydrate crystallization point. When single crystals were grown at higher driving force, in supercooled conditions at 0°C (Fig. 2.5E) or at -1.5°C , they exhibited a skeletal morphology like the crystals grown in AFPs and PVP.

AFPs and Gas Hydrates

Gas hydrates were formed under high driving force using a methane/ethane/propane gas mixture so as to produce sII hydrate (Fig. 2.6). Both average nGas and average consumption rates followed identical patterns. Because the pure sample stopped growing at approximately 1,500 min, we chose this time as a cutoff point to compare nGas and growth rates. On average,

the highest level of inhibition was seen in the presence of Type III AFP (with no GFP fusion protein), which consumed 6.0 mmol of gas and decreased hydrate growth rate by 18% compared to the pure water control samples, which consumed the highest amount of gas at 7.4 mmol and had the fastest growth rate. LpAFP-GFP and Type III AFP-GFP also showed consumption inhibition (6.6 mmol < gas consumption < 6.4 mmol) with growth rate inhibition ranging from 10 to 13%. In contrast, after the control, the GFP and PVP samples showed the highest levels of gas consumption, at 6.9 mmol and the lowest growth rate inhibition of 7.1%.

Discussion

The observation that the polycrystalline THF hydrates are strikingly fluorescent after being grown in the presence of recombinant AFP-GFPs (Fig. 2.3) is irrefutable evidence that these proteins adsorb to sII hydrates. Further substantiation is provided by the morphological changes on single hydrate crystals mediated by these same proteins (Fig. 2.5). This might not have been predicted *a priori* because although hydrates have an ice-like appearance, their structure is markedly different. Under common conditions, water freezes into hexagonal ice (Ih), taking the form of a hexagonal prism with two basal faces and six rectangular prism faces.²¹ Moderately active AFPs such as Type III AFP (and Type III AFP-GFP) have been shown to bind to the ice basal planes, and the low activity LpAFP binds to the prism planes.^{22,23} Thus, evolutionary forces have shaped these AFPs so that they fit snugly to these ice surfaces making it more energetically expensive for water molecules to join the growing ice lattice. In contrast, sII hydrates have a symmetrical cubic structure and therefore, although similarly flat to ice, present geometrically-distinct, but uniform surfaces for AFP adsorption.

There was no preference by AFPs for any of the 8 identical {111} hydrate faces (Fig. 2.5C), and indeed the resulting hopper like crystals were similar to those generated in the presence of the commercial kinetic inhibitor, PVP (Fig. 2.5D). This skeletal growth is believed to occur as a result of the more efficient dissipation of the heat of crystallization on the crystal edges, as opposed to the interior planes, as has been previously described.¹⁵ At higher driving forces (4.4 and 5.9 °C subcooling), we demonstrated that these faces were the slowest growing regions of the crystal. Since GFP alone did not adsorb to the THF hydrate (Figs. 2.3 and 2.4), we postulate that the inhibition of hydrate growth by AFPs is mediated by the structure of the proteins, and these become adsorbed into the crystal below the equilibrium growth point. Curiously perhaps, the plant LpAFP-GFP with low TH activity towards ice, showed 1.6 fold more absorption into polycrystalline THF hydrate (at least at the higher concentrations) than the moderately ice active Type III AFP-GFP. However, Type III without the GFP tag appeared to have superior hydrate-shaping, but its hydrate-binding affinity could not be quantified due its vulnerability to THF denaturation at higher concentrations.

Since these experiments were all conducted with the model THF hydrate, we thought it important to demonstrate that these recombinant proteins also showed inhibition toward natural gas hydrates. Although some fish AFPs and insect AFPs have shown activity as hydrate inhibitors in propane hydrate,²⁴ these particular GFP fusions have never been tested, nor have the tested hydrates been formed using a gas mixture that would be found in a high-pressure oil and gas pipeline.²⁵ All of the investigated AFPs showed hydrate inhibition as determined by gas uptake assessments. Similar to the observations on the single THF crystals, LpAFP-GFP and Type III AFP-GFP showed hydrate inhibition that was higher but nonetheless comparable to the chemical inhibitor PVP, which along with GFP showed the lowest inhibition. Of the additives

tested, Type III AFP was demonstrably superior with an overall 18% decrease in gas hydrate formation, and again validating the observations made with the THF hydrate single crystals.

In conclusion, we have demonstrated for the first time that AFPs adsorb to sII hydrate surfaces and we speculate that they act as inhibitors by binding to the {111} faces of these symmetrical cubic crystals. We further consider that the identified ice-binding residues of these proteins may not be identical to the residues that interact with the hydrate surface, but the way is now clear for such an investigation. In addition, these experiments have established that AFPs are suitable models for understanding hydrate-inhibitor reactions and offer the prospect that these proteins, or their modified cognates, will be useful as new and more effective biologically-based hydrate inhibitors.

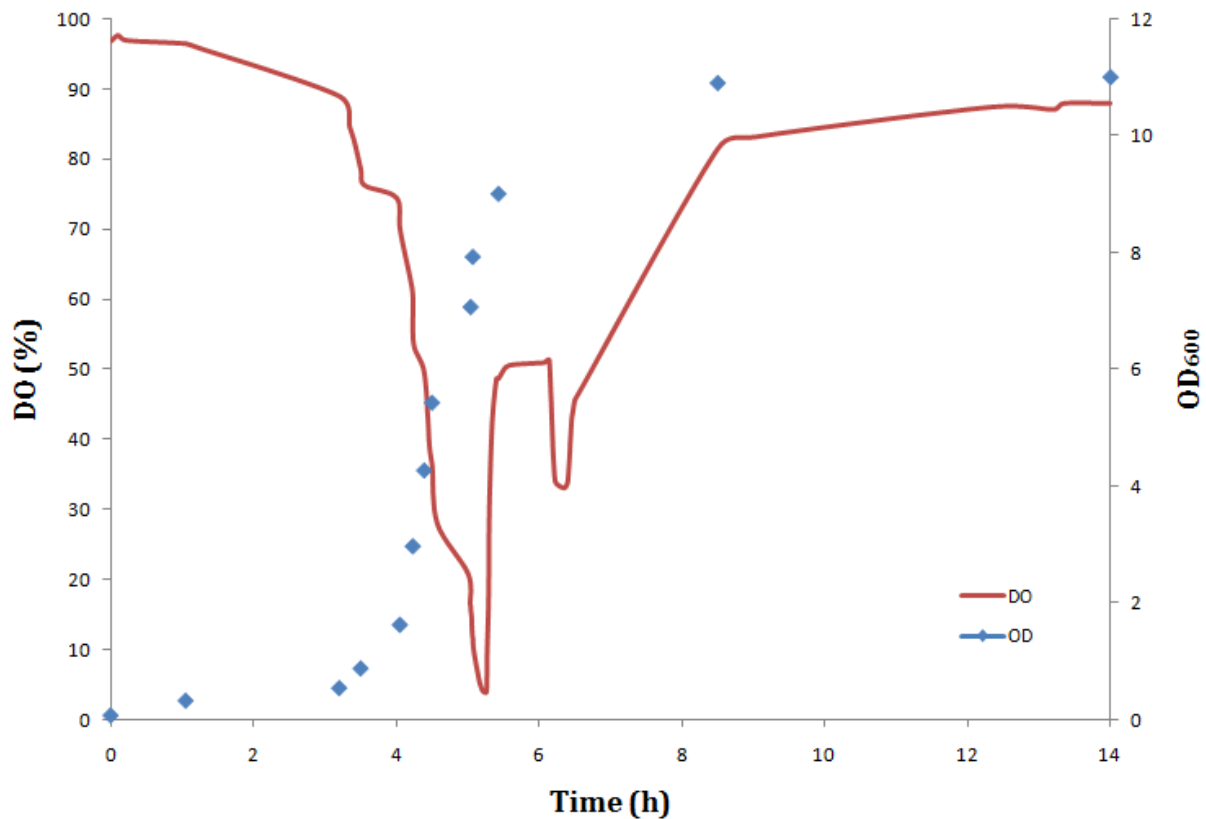


Figure 2.1. A typical DO/OD₆₀₀ trend for *E. coli* BL21 expressing recombinant proteins, shows a drop in DO levels as a result of increased bacterial growth (rising OD₆₀₀) and subsequent oxygen utilization at 37°C. At the exponential growth phase, when DO levels drop to their lowest (0-20%), the culture is induced with IPTG and the temperature is lowered ($\leq 20^\circ\text{C}$). The OD is calculated spectrophotometrically at 600 nm.

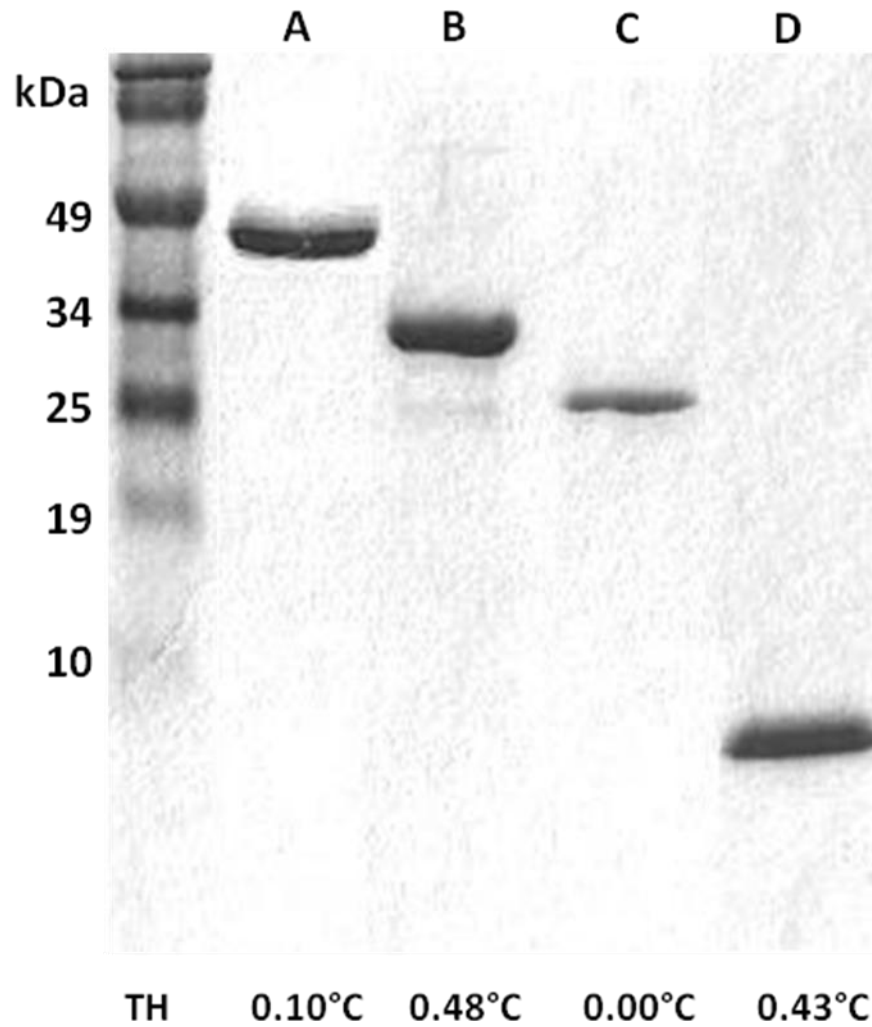


Figure 2.2. Purification of Recombinant Proteins. 12% SDS-PAGE analysis of recombinant His-tagged proteins LpAFP-GFP (A), Type III AFP-GFP (B), GFP (C) and Type III AFP (D), purified using Co^{2+} -agarose affinity chromatography. TH values are shown below.



Figure 2.3. Adsorption of AFPs on THF hydrate. THF hydrate polycrystals fluoresce green under UV light after being grown in solutions containing Type III AFP-GFP (left) and LpAFP-GFP (center). THF hydrate crystals grown in GFP control solutions (right) do not fluoresce. Sample diameters were 3 – 3.5 cm.

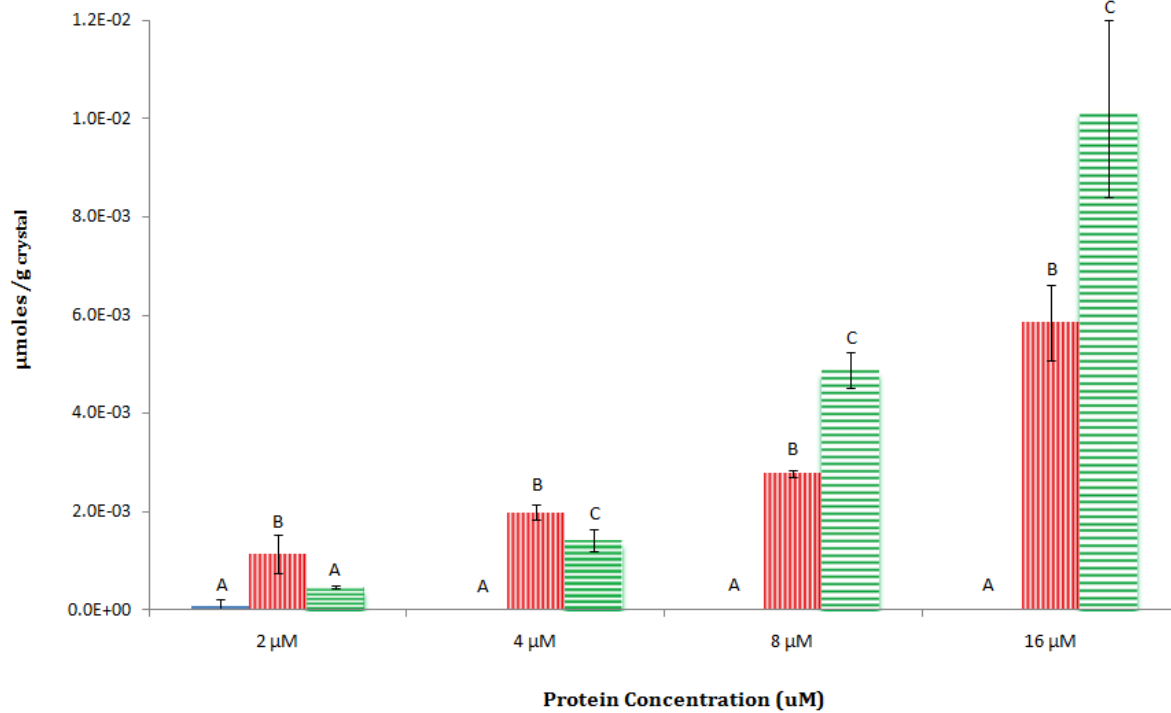


Figure 2.4. Differences in the average μmoles of protein adsorbed per gram of THF hydrate crystal ($\mu\text{moles}/g_{\text{crystal}}$) between LpAFP-GFP (horizontal lines), Type III AFP-GFP (vertical lines) and GFP (solid) are plotted as a function of protein concentration (μM) in a solution containing THF (3.34:1, v/v, protein solution:THF). Bars indicate standard deviation. Statistical significance between each data group is indicated by letters A-C, where identical letters indicate no statistical difference.

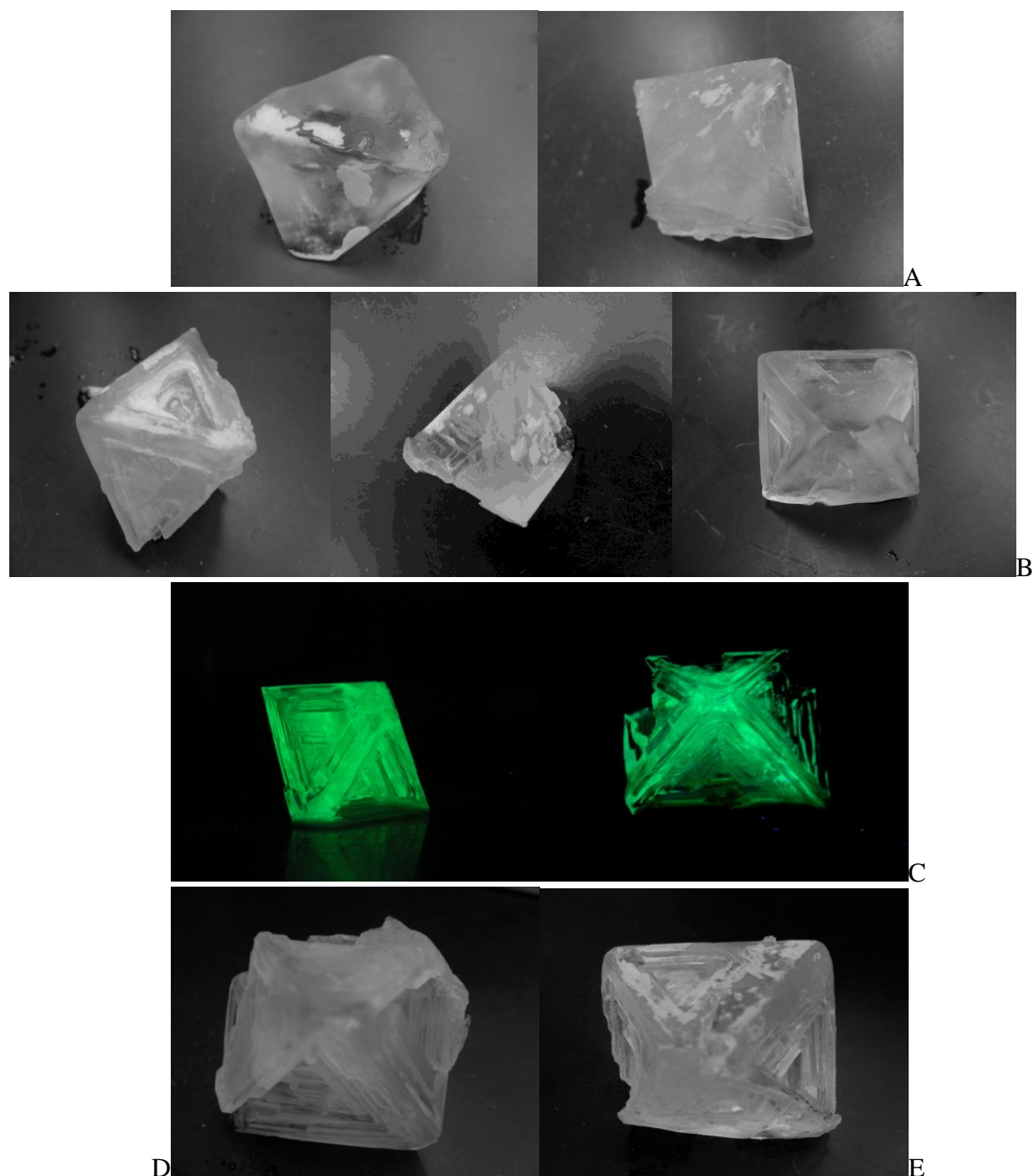
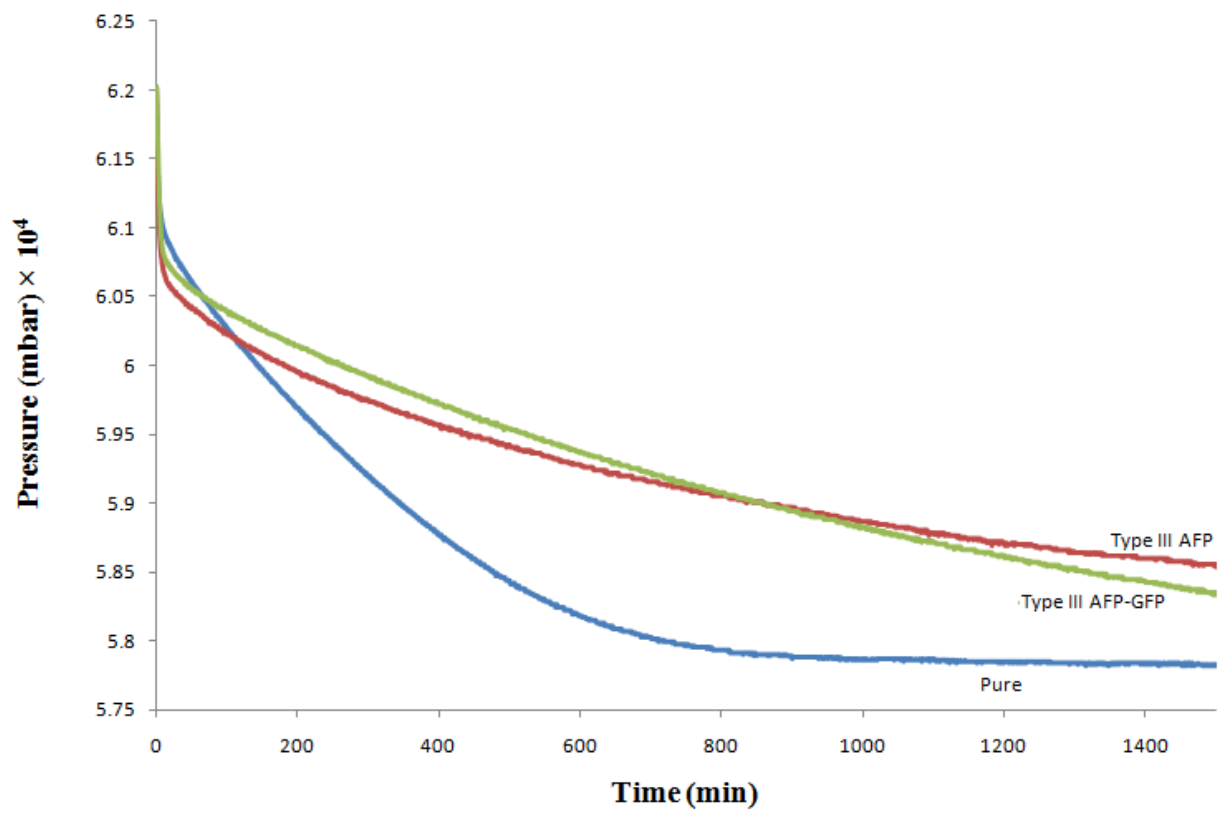
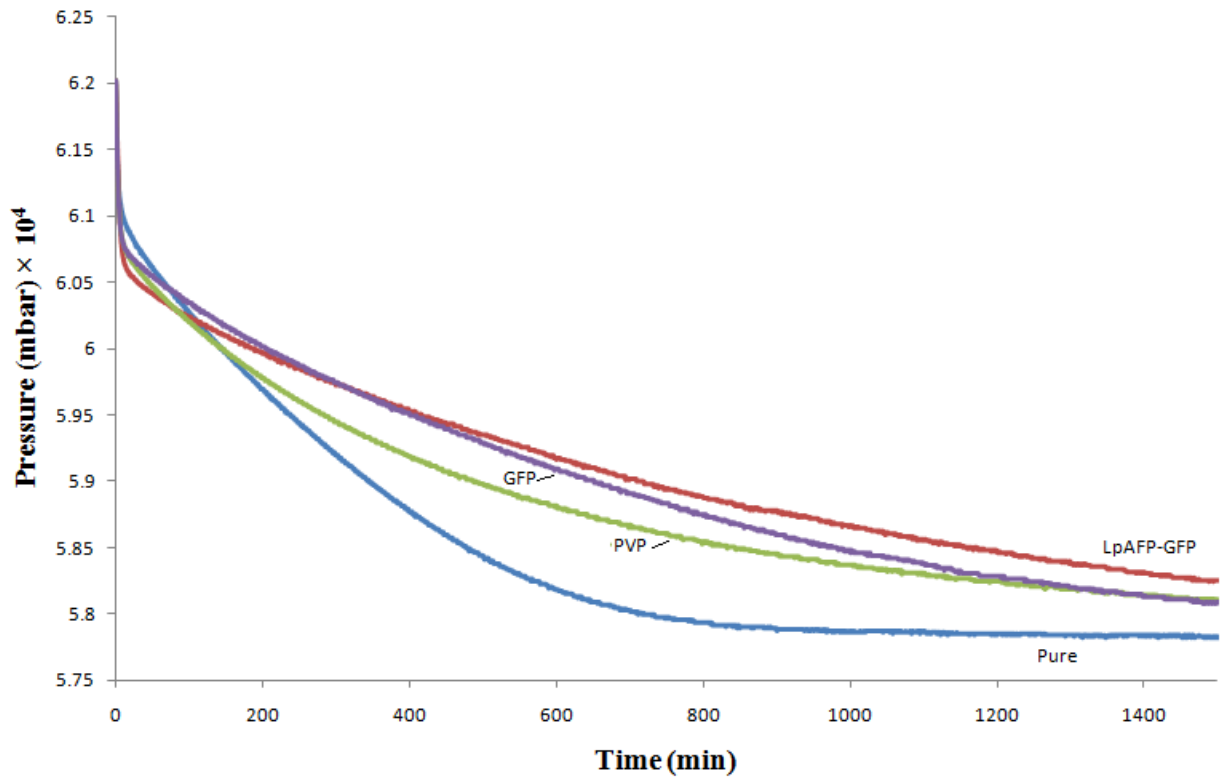


Figure 2.5. Single THF hydrate Crystals grown at 3°C. (A) Unmodified crystals grown from pure THF/water and 200 µg/ml GFP. (B) Skeletal Crystals grown in solutions with 200 µg/ml Type III AFP (left), 200 µg/ml LpAFP-GFP (center) and 15 µg/ml Type III AFP (right). (C) Crystals with adsorbed 100 µg/ml Type III AFP-GFP (left) and LpAFP-GFP (right) fluoresce under UV light. (D) Skeletal crystal grown in 200 µg/ml PVP. (E) Skeletal crystal grown at 0°C from pure THF/water. Crystal diameters are 4.5-5 cm.



A



B

Figure 2.6. Pressure summary of sII methane/ethane/propane gas hydrate. Absolute pressure drops indicate the moles of gas consumed with various additives at 0.1 mM. **(A)** Pressure trends for Type III AFP and LpAFP-GFP. **(B)** Pressure trends for Type III AFP-GFP, GFP, PVP and pure sample. Slopes of the curves indicate rates of gas consumption.

References

1. Sloan, D. E. and Koh, A. C. (2007) Clathrate Hydrates of Natural Gases, 3rd Ed. Boca Raton, FL: CRC Press.
2. Berez, E. and Balla-Achs, M. (1983) Gas Hydrates, Studies in Inorganic Chemistry 4. New York, NY. Elsevier Science Publishing Co., Inc.
3. Makogon, Y. T., Larsen, R. Knight, A. C. and Sloan, D. E. (1997) Melt growth of tetrahydrofuran clathrate hydrate and its inhibition: method and first results. *Journal of Crystal Growth* **179**, 258-262.
4. Davies, R. S., Selim, S. M., Sloan, D. E., Bollavaram, P. and Peters, J. D. (2006) Hydrate Plug Dissociation. *American Institute of Chemical Engineers Journal* **52**, 4016.
5. Mehta, A., Walsh, J. and Lorimer, S. (2006) Hydrate Challenges in Deep Water Production and Operation. *Annals of the New York Academy of Sciences* **912**, 366-373.
6. Koh, A. C., Westacott, E. R., Zhang, W., Hirachand, K., Creek, L. J. and Soper, K. A. (2002) Mechanisms of gas hydrate formation and inhibition. *Fluid Phase Equilibria* **30**, 143-151.
7. Lederhos, P. L., Long, P. J., Sum, A., Christiansen, L. R. and Sloan Jr., D. E. (1996) Effective kinetic inhibitors for natural gas hydrates. *Chemical Engineering Science* **51**, 1221-1229.
8. Huo, Z., Freer, E., Lamar, M., Sannigrahi, B., Knauss, M. D. and Sloan Jr., D. E. (2001). Hydrate plug prevention by anti-agglomeration. *Chemical Engineering Science* **56**, 4979-4991.
9. Scholander, F. P., Gordon, M. S. and Ben, H. Freezing Resistance in Some Northern Fishes. *Amdur Biological Bulletin* **122**, 52-62.
10. Gilbert, A. J., Davies, L. P. and Laybourn-Parry, J. (2005) A hyperactive, Ca²⁺-dependent antifreeze protein in an Antarctic bacterium, *FEMS Microb. Lett.* **245**, 67-72.
11. Middleton, J. A., Brown, M. A., Davies, L. P. and Walker, K. V. (2009) Identification of the ice-binding face of a plant antifreeze protein. *Federation of the Societies of Biochemistry and Molecular Biology Letters* **583**, 815-819.
12. Tyshenko, G. M., Doucet, D., Davies, L. P. and Walker, K. V. (1997) The antifreeze potential of the spruce budworm thermal hysteresis protein. *Nature* **15**, 887-890.
13. Barrett, J. (2001) Thermal hysteresis proteins, *The International Journal of Biochemistry & Cell Biology* **33**, 105-117.
14. Zeng, H., Wilson, D. L., Walker, K. V. and Ripmeester, A. J. (2006) Effect of Antifreeze Proteins on the Nucleation, Growth, and the Memory Effect during Tetrahydrofuran Clathrate Hydrate Formation. *Journal of American Chemical Society* **128**, 2844-2850.

15. Larsen, R., Knight, A. C., Sloan, D. E. (1998) Clathrate hydrate growth and inhibition. *Fluid Phase Equilibria*, **150**, 353-360.
16. Chakrabartty, A. and Hew, C. L. (1991) The effect of enhanced α -helicity on the activity of a winter flounder antifreeze polypeptide. *European Journal of Biochemistry* **202**, 1057-1063.
17. Knight, A.C. and Rider, K. (2002) Free-growth forms of tetrahydrofuran clathrate hydrate crystals from the melt: plates and needles from a fast-growing vicinal cubic crystal. *Philosophical Magazine A* **82**, 1609-1632.
18. Seo, Y. Ripmeester, A. J., Lee, J. and Lee, H. (2005) Efficient Recovery of CO₂ from Flue Gas by Clathrate Hydrate Formation in Porous Silica Gels. *Environmental Science Technology* **39**, 2315-2319.
19. Lee, D. J. and Englezos, P. (2005) Enhancement of the performance of gas hydrate kinetic inhibitors with polyethylene oxide. *Chemical Engineering Science* **60**, 5323-5330.
20. Smith, H. C., Van Ness, C. H. and Abbott, M. M. (2001) Introduction to Chemical Engineering Thermodynamics. McGraw-Hill, New York, NY
21. Materer, N., Starke, U., Barbieri, M., van Hove, A., Somorjai, G. A., Kroes, J. G. and Minot, C. (1995) Molecular Surface Structure of a Low-Temperature Ice Ih(0001) Crystal. *Journal of Physical Chemistry* **99**, 6267-6269.
22. Scooter, J. A., Marshall, C. B., Graham, A. L., Gilbert, A. J., Garnham, P. C. and Davies, L. P. (2006) The basis for hyperactivity of antifreeze proteins. *Cryobiology* **53**, 229-239.
23. Pudney, A. D. P., Buckley, L. S., Sidebottom, M. C., Twigg, N. S., Sevilla, P. M., Holt, B. C., Roper, D., Telford, H. J., McArthur, J. A. and Lillford, J. P. (2002) The physic-chemical characterization of a boiling stable antifreeze protein from a perennial grass (*Lolium perenne*). *Archives of Biochemistry and Biophysics* **410**, 238-245.
24. Zeng, H., Moudrakovski, L. I., Ripmeester, A. J. and Walker, K. V. (2006) Effect of antifreeze protein on nucleation, growth and memory of gas hydrates. *American Institute of Chemical Engineers* **54**, 3304-3309.
25. Kennedy, L. J. (1993) Oil and gas pipeline fundamentals, 2nd Ed. Pennwell Corp. Tulsa, OK.

Chapter 3

Tetrahydrofuran Hydrate Inhibition Using Cold-Adapted Bacteria

Raimond Gordienko*, Hiroshi Ohno† and Virginia K. Walker*.

Departments of Biology*, Queen's University, Kingston ON, K7L 3N6, Canada. Materials Structure and Function Group†, National Research Council Canada, Ottawa ON, K1A 0R6, Canada.

Abstract

The use of antifreeze proteins (AFPs) as potential inhibitors of unscheduled gas hydrate formation has been explored. However, the difficulty and expense of purifying recombinant AFPs is unlikely to make them a practical solution for the petroleum industry. We have investigated the use of cold-adapted bacteria for this application. We have identified certain isolates with the ability to adsorb to tetrahydrofuran (THF) hydrate and inhibit the growth rate more effectively than isolates with lower hydrate-binding affinity. Inhibition of high-pressure methane/ethane/propane hydrate using bacteria was also tested but did not prove as effective as with THF hydrate. Overall, however, there is a link between levels of bacterial-hydrate adsorption and inhibition similar to those observed with AFPs and hydrates. This may facilitate the future development of ice-associating bacteria as novel agents for controlling hydrate formation in the field.

Introduction

Natural gas hydrates are a class of clathrate compounds that form at low temperatures and high pressures, consisting of light hydrocarbons such as methane, ethane and propane, trapped in a surrounding hydrogen-bonded water cage of appropriate diameter.¹ In the oil and gas industry, gas hydrate formation in flowlines has been known to block product flow, damage production facilities, and if not properly removed, lead to safety hazards for personnel.² For over half a century, thermodynamic inhibitors, such as alcohols and glycols have been used to prevent and control gas hydrate formation.³ Nevertheless, a more recent shift has been observed from thermodynamic inhibitors to sometimes cheaper, less hazardous and environmentally-safe alternatives. Amongst them are kinetic inhibitors; molecules that bind to hydrate crystals and interfere with the nucleation and growth of the crystals, and antiagglomerants; chemicals with polar and non-polar groups that keep hydrate crystals dispersed in the hydrocarbon phase, preventing their aggregation.^{4,5}

We have shown that antifreeze proteins (AFPs) have potential as a new class of biologically-based hydrate inhibitors that function in a similar fashion to the commercial kinetic inhibitor poly-N-vinylpyrrolidone (PVP).^{6,7} Because production of purified recombinant AFPs is unlikely to be cost-effective for industrial-scale usage, we wished to investigate the potential use of cold-adapted microorganisms as hydrate inhibitors. Some microorganisms including the soil bacteria *Carnobacterium* sp., *Acinetobacter* sp. and *Buttiauxella* sp. have the ability to tolerate the stress associated with multiple freeze-thaw cycles,⁸ while lysates from bacteria like *Flavobacterium* sp., *Chryseobacterium* and Antarctic α and γ - *Proteobacteria* have been shown to inhibit the recrystallization of ice, a process where larger ice crystals grow at the expense of smaller ones.⁹⁻¹¹ Moreover, cryoprotection is further aided by other mechanisms such as

modified membrane lipids, polysaccharides and ice-associating proteins including ice-nucleating proteins and antifreeze proteins.¹² Only a few bacteria have been shown to possess AFP activity including *Moraxella* sp., *P. putida*, *R. erythropolis*, *M. cryophilus* and *M. primoryensis*,¹³⁻¹⁵ with many of these isolates from polar regions.

Here we examine if some of these cold-adapted bacteria have the ability to bind to and inhibit hydrate growth using a model tetrahydrofuran (THF) hydrate as well as high pressure methane/ethane/propane hydrate. If there is a link between bacterial adsorption to THF hydrate and inhibition, the bacteria may serve as suitable growth inhibitors of both THF and methane/ethane/propane hydrates.

Materials and Methods

Bacterial Strains and THF solutions

Freeze-thaw tolerant bacteria *Chryseobacteria* sp. C14, *Buttiauxella* sp. G2b1, the ice-associating *P. putida* UW4, as well as freeze-intolerant control *E. coli* BL21 were grown from a single colony in 1L flasks containing 10% Tryptic Soy Broth (TSB; BD Bioscience, Sparks, MD, USA), 0.1 g (NH₄)₂SO₄, 0.1 g KNO₃ and 0.1 g K₂HPO₄, with shaking for two days. All strains were grown at room temperature except *E. coli*, which was grown at 37°C. Prior to experimentation, bacteria were placed at 4°C for 12 h to induce the expression of any cold-adapted proteins that may be produced as a response to low temperatures.

THF (≥99.5%, Sigma-Aldrich, St. Louis, MO, USA) was mixed with bacterial cultures at 1:3.34, (v/v, THF:culture) as previously described.⁶

Bacteria and THF Hydrate

Survival in THF was tested by subjecting bacterial cultures to THF at 1:3.34 (v/v) in a 1 ml microcentrifuge tube at 4°C for 2, 4 and 8 h. Subsequently, 50 µl of a 10² dilution of the culture solution was plated on 10% TSB and incubated at room temperature for 2 days and the presence of any bacterial colonies was noted. Any changes to bacterial morphology following THF exposure was determined by microscopic examination (Nikon Eclipse E600) and photographically recorded using a mounted digital camera (Nikon QImaging QICAM). Additives including salts (NH₄HCO₃, NH₄Cl and CaCl₂, tested at 0.02 g/ml) and detergents (sodium dodecyl sulfate (SDS) and Triton X-100 (Fisher BioReagents, Ottawa, ON), at 0.06%, w/v) were tested on THF-exposed bacteria to establish their effectiveness against bacterial aggregation. Survival in Triton X-100 was also tested by incubating the bacterial cultures with 0.06 % (w/v) Triton X-100 and plating 50 µl of the culture as indicated.

Effects of bacteria on the polycrystalline THF hydrate growth was determined by monitoring the formation of polycrystalline THF hydrate from a THF/10% TSB bacterial culture containing 0.06% Triton X-100. A cooled brass finger was used as previously described,⁶ starting from an initial temperature of 2°C and a final temperature of -4.5°C (with a 0.5°C drop every 30 min). Two different bacterial concentrations were used; 400 million cells/ml (low concentration) and 1.5 billion cells/ml (high concentration). Bacterial counts were assessed using standard curves (Appendix C). When complete, the crystal was removed as previously described and weighed.⁶ The average rate of growth in grams per hour (g/h), was then calculated and compared to the control (a solution of THF/water and 0.06% (w/v) Triton X-100). Bacterial adsorption was established by melting the crystal and centrifuging the melt for 20 min at 3000 × g, and re-suspending the bacterial pellet with 1 ml of 10% TSB. The optical density at 600nm

(OD₆₀₀) of the sample was then determined and the value was used as an estimate of adsorbed cell density in each crystal melt. All statistical analyses were performed using a Tukey-Kramer test.

Bacteria and sII gas Hydrate

Bacteria were mixed at 400 million cells/ml with 1000 Å silica gel (Silicycle Chemicals, St. Jean-Baptiste, QC), added into a stainless steel cell, purged twice and pressurized to 1000 PSI (6.9×10^4 mbar) using a natural gas mix consisting of 93% methane, 5% ethane and 2% propane (Linde Canada, Mississauga, ON) allowing for sII hydrate formation at 0.5°C, as previously illustrated.⁶

Results and Discussion

THF is highly toxic to bacteria,¹⁶ and the isolates used here were no exceptions; no colonies formed on plates after cultures were subjected to THF for any time period (results not shown). Although unable to divide, the cells appeared to remain intact as whole cells (Fig. 3.1.A). Of the strains used in these experiments, *Chryseobacteria* sp. C14 and *E. coli* formed aggregates as a result of THF exposure (Fig. 3.1.A). We hypothesized that the observed aggregation could interfere in any interaction with THF hydrate and therefore to limit aggregation, salts and detergents were added to the THF-containing cultures. While none of the salts reduced clumping, the surfactants SDS and Triton X-100 were effective. Of the two surfactants, Triton-X100 proved most practical (Fig. 3.1.B), and therefore was routinely used. These results are in concordance with previous studies on the use of Triton X-100 to loosen biofilms and to prevent bacterial adherence.^{17,18} It should be noted that although Triton X-100 is

commonly used to lyse cells at 1% w/v,¹⁹ it did not cause lysis or a significant reduction in the bacterial colonies used here at 0.06% w/v (results not shown).

Similar to our previous findings that AFPs adsorb into THF hydrate,⁶ we found that certain bacteria also adsorbed to hydrate (Fig. 3.2). At low bacterial concentrations, *P. putida* UW4 (OD₆₀₀ = 1.4), *Chryseobacteria* sp. C14 and *E. coli* (OD₆₀₀ = 1.2 and 1.6, respectively) all showed relatively similar levels of adsorption, while *Buttiauxella* sp. G2b1 (OD₆₀₀ = 0.58) displayed the lowest level of adsorption. Since there was no significant difference between these, with *Buttiauxella* G2b1 as the only exception, higher concentrations of bacteria were tested. As expected, levels of adsorption were higher at the elevated concentrations, with *P. putida* UW4 and *Buttiauxella* sp. G2b1 both showing adsorption levels of OD₆₀₀ > 5.3. They were significantly higher than the adsorption levels of *E. coli* and *Chryseobacteria* sp. C14, which showed lower OD₆₀₀ values of 4.3 and 3.3, respectively. The low adsorption levels in *Chryseobacteria* sp. C14 could be as the result of its tendency to form the largest aggregates, even in the presence of Triton X-100 (Fig. 3.1.A). Since the cells with the highest adsorption levels have known ice-associating properties, and one of which (*Buttiauxella* sp. G2b1) has been shown to adhere to ice from a consortium,⁸ it is possible that the polycrystalline THF hydrate reflects these characteristics.

When THF hydrate growth rates were compared, *P. putida* UW4 exhibited the best inhibition of the strains at low concentration (Fig. 3.3), with over a 24% reduction in the rate of growth, compared to the control. This level of inhibition was only observed when bacterial strains were used at high concentrations of 1.5 billion cells/ml, where reduction of THF hydrate growth rates ranged from 20 to 29%. After *P. putida* UW4 at low concentrations, *Buttiauxella* sp. G2b1 inhibited hydrate growth by 17%, followed by a 12% with *E. coli*. Although

Chryseobacterium sp. C14 has previously been noted to delay THF hydrate nucleation,²⁰ in this work, it appeared to promote hydrate growth, showing higher levels of growth rate than the control. At high cell-densities, there appears to be a link between the levels of adsorption and extent of inhibition, similar to that seen with AFPs and hydrates.⁶ In summary, *P. putida* UW4 and *Buttiauxella* sp. G2b1 showed the highest levels of adsorption and were the best inhibitors compared to *E. coli* and *Chryseobacteria* sp. C14 which showed the lowest adsorption and were the weakest inhibitors.

Since *P. putida* UW4 demonstrated the most effective THF hydrate growth inhibition at 400 million cells/ml, we assessed its performance in high-pressure hydrate experiments. It did not show a reduction in gas consumption (Fig. 3.4), with 6.4 mmoles of gas consumed, compared to 6.6 mmoles in the control (10% TSB). The gas consumption curves followed similar trends, indicating that there was no inhibition of growth rate with the bacteria. It is possible that this negative result may be due to a non-homogenous mix of bacteria in the silica gel. Typically, rod-shaped bacterial are 2 μm in diameter (20,000 \AA),²¹ much larger than the pore diameter of the silica gel matrix (1000 \AA). As a result, most of the solution inside the silica gel may not have come in contact with bacteria, which were likely scattered on the outside of the silica gel matrix. This may have constrained any putative inhibition mediated by *P. putida* UW4 as it would have only been able to bind to hydrate on the peripheral sections of the silica gel.

In conclusion, there appears to be a relationship between bacterial hydrate adsorption and inhibition where bacteria that adsorb to hydrate crystals inhibit the growth more effectively than ones with less hydrate binding affinity. Moreover, although THF hydrate results indicated that of the four strains, *P. putida* UW4 was the most effective at slowing hydrate growth rate, results with the high-pressure system did not show a comparable outcome most likely for technical

reasons. Future work with this system may require the use of silica gels with larger pore diameters or stirred reactors.

Along with the previous work using AFPs, these results show that THF hydrate can be inhibited by biologically-based materials that adsorb to hydrate surfaces. The way is now clear to develop a system to adequately test these as natural gas hydrate inhibitors.

References

1. Koh, A. C. (2002) Towards a fundamental understanding of natural gas hydrates. *The Chemical Society Reviews* **31**, 157-167.
2. Mehta, A., Walsh, J. and Lorimer, S. (2006) Hydrate Challenges in Deep Water Production and Operation. *Annals of the New York Academy of Sciences* **912**, 366-373.
3. Koh, A. C., Westacott, E. R., Zhang, W., Hirachand, K., Creek, L. J. and Soper, K. A. (2002) Mechanisms of gas hydrate formation and inhibition. *Fluid Phase Equilibria* **30**, 143-151.
4. Makogon, Y. T. and Sloan, D. E. (2002) Mechanisms of Kinetic Hydrate Inhibitors, Proc 4th International Hydrate Conference, Yokohama, Japan.
5. Gao, S. (2009) Hydrate Risk Management at High Watercuts with Anti-agglomerant Hydrate Inhibitors. *Energy and Fuels* **23**, 2118-2121.
6. Gordienko, R., Ohno, H., Singh, K. V., Zhongchao, J., Ripmeester, J. and Walker, K. V. (2009) Towards a Green Hydrate Inhibitor: Imaging Antifreeze Proteins on Clathrates. (*In preparation*).
7. Zeng, H., Moudrakovski, L. I., Ripmeester, A. J. and Walker, K. V. (2006) Effect of antifreeze protein on nucleation, growth and memory of gas hydrates. *American Institute of Chemical Engineers* **54**, 3304-3309.
8. Walker, K. V., Palmer, R. G. and Voordouw, G. (2006) Freeze-Thaw Tolerance and Clues to the Winter Survival of a Soil Community. *Applied and Environmental Microbiology* **72**, 1784-1792.
9. Chattopadhyay, K. M. (2002) Bacterial Cryoprotectants, *Resonance* **7** 59-63.
10. Gilbert, A., J., Hill, J. P., Dodd, R. E. C., Layborn-Parry, J. (2004) Demonstration of antifreeze protein activity in Antarctic lake bacteria. *Microbiology* **150**, 171-180.
11. Hon, C. W., Griffith, M., Mlynarz, A., Kwok, C. Y. and Yang, C. S. D. (1995) Antifreeze Proteins in Winter Rye Are Similar to Pathogenesis-Related Proteins. *Plant Physiology* **109**, 879-889.
12. Kawahara, H. (2008) Psychrophiles: from Biodiversity to Biotechnology, Germany: Springer-Verlag Berlin Heidelberg.
13. Yamashita, Y., Nakamura, N., Omiya, K., Nishikawa, J., Hidehisha, K. and Obata, H. (2002) Identification of an Antifreeze Lipoprotein from *Moraxella* sp. of Antarctic Origin. *Bioscience, Biotechnology and Biochemistry* **66**, 237-247.

14. Xu, H., Griffith, M., Patten, C. L. and Glick, B. R. (1998). Isolation and characterization of an antifreeze protein with ice nucleation activity from the plant growth promoting rhizobacterium *Pseudomonas putida* GR12-2. *Can J Microbiol* **44**, 64–73.
15. Gilbert, A. J., Davies, L. P. and Laybourn-Parry, J. (2005) A hyperactive, Ca²⁺-dependent antifreeze protein in an Antarctic bacterium, *FEMS Microb. Lett.* **245**, 67-72.
16. Huva, E.I. 2006. Microbial Nucleation and Inhibition of Tetrahydrofuran Hydrate. Undergraduate Thesis. Department of Biology, Queen's University, Kingston, Ontario.
17. De Carvalho, R. C. C. (2007) Biofilms: Recent Developments on an Old Battle. *Recent Patents on Biotechnology* **1**, 49-57.
18. Stelmack, L. P., Gray, R. M. and Pickard, A. M. (1999) Bacterial Adhesion to Soil Contaminants in the Presence of Surfactants. *Applied and Environmental Microbiology* **65**, 163-168.
19. Goswami, T. and Andrews, C. N. (2006) Hereditary Hemochromatosis Protein, HFE, Interaction with Transferrin Receptor 2 Suggests a Molecular Mechanism for Mammalian Iron Sensing. *Journal of Biological Chemistry* **39**, 28494-28498.
20. Huva, Emily I.; Gordienko, Raimond V.; Ripmeester, John A.; Zeng, Huang; Walker, Virginia K. 2008. The Search for “Green Inhibitors”: Perturbing Hydrate Growth with Bugs. Proceedings of the 6th International Conference on Gas Hydrates, Vancouver, BC, Canada, July 6-10, 2008.
21. Nelson, L. D. and Cox, M. M. (2005) *Lehninger Principles of Biochemistry*, 4th Ed. NY: W.H. Freeman and Company.

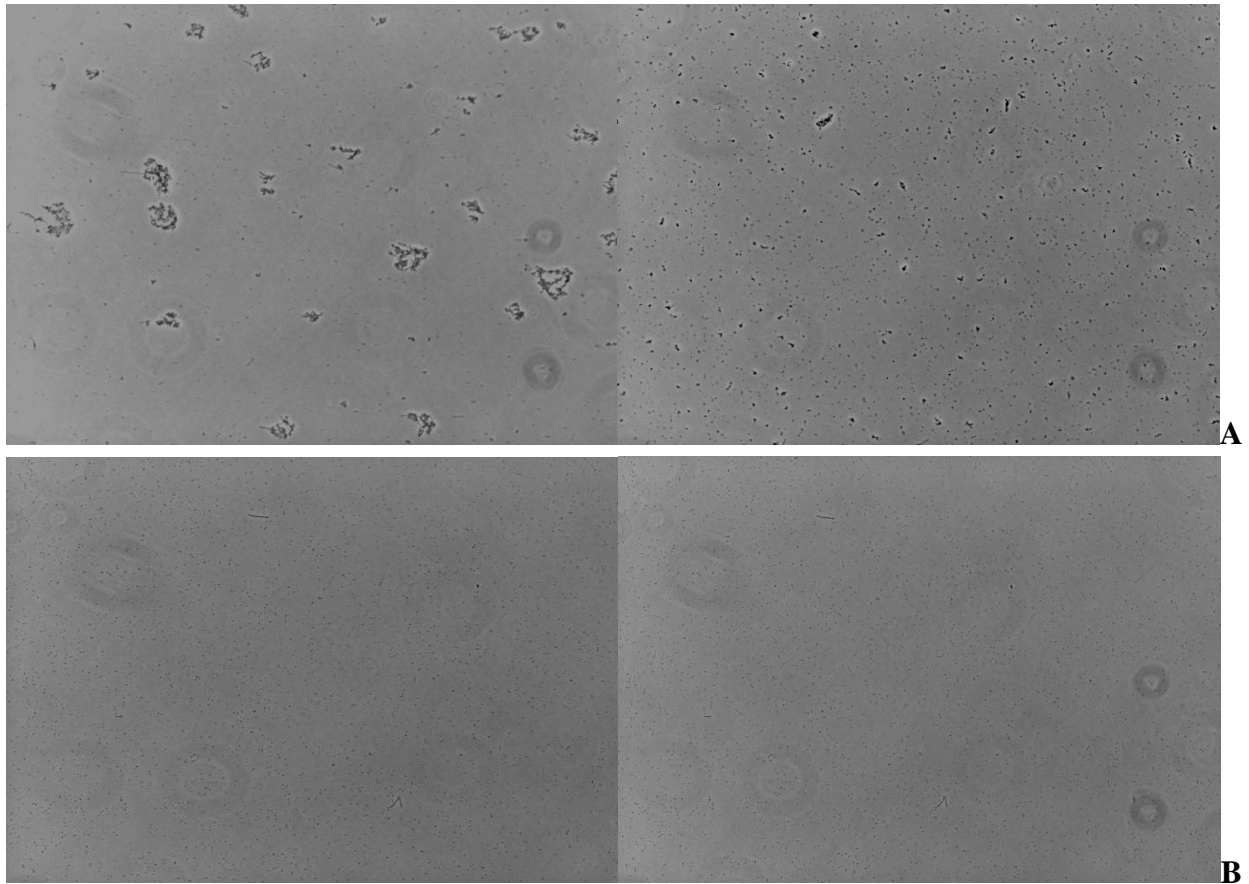


Figure 3.1. Bacteria in THF: pre and post Triton X-100 Treatment (Magnification 400×). (A) At 400 million cells/ml, *Chryseobacteria* sp. C14 (left) and *E. coli* (right), form aggregates when exposed to THF. (B) Cultures as described in (A) mixed with 0.06% Triton X-100 in the presence of THF did not aggregate as severely; *Chryseobacteria* sp. C14 (left) and *E. coli* (right).

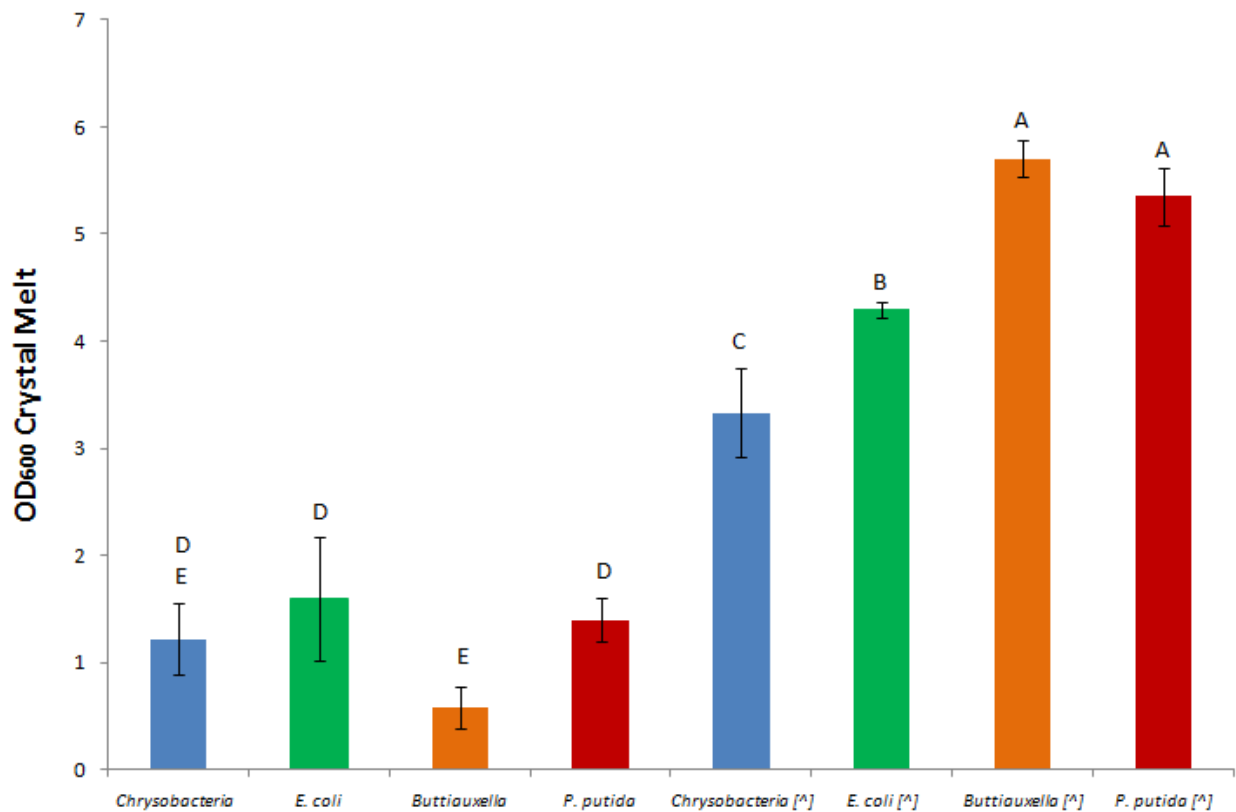


Figure 3.2. Bacterial adsorption into THF hydrate. Amounts of adsorbed bacteria in the crystal melt are displayed on the y-axis as OD₆₀₀. Bacterial concentrations in THF/culture solutions were 400 million cells/ml, [^] indicates a bacterial concentration of 1.5 billion cells/ml. Different letters above the bar indicate statistical significance.

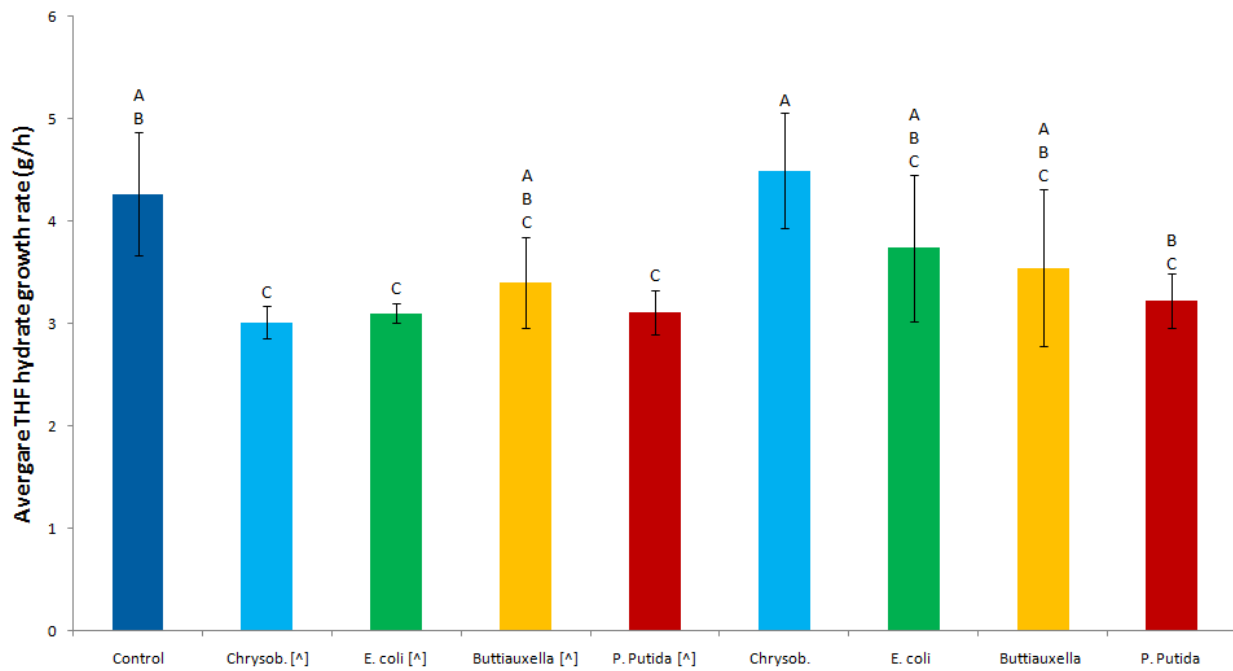


Figure 3.3. THF hydrate growth rate. Growth rate of THF hydrate in bacterial cultures, measured in g/h. Bacterial concentrations are 400 million cells/ml, [^] indicates a bacterial concentration of 1.5 billion cells/ml. Different letters indicate statistical significance.

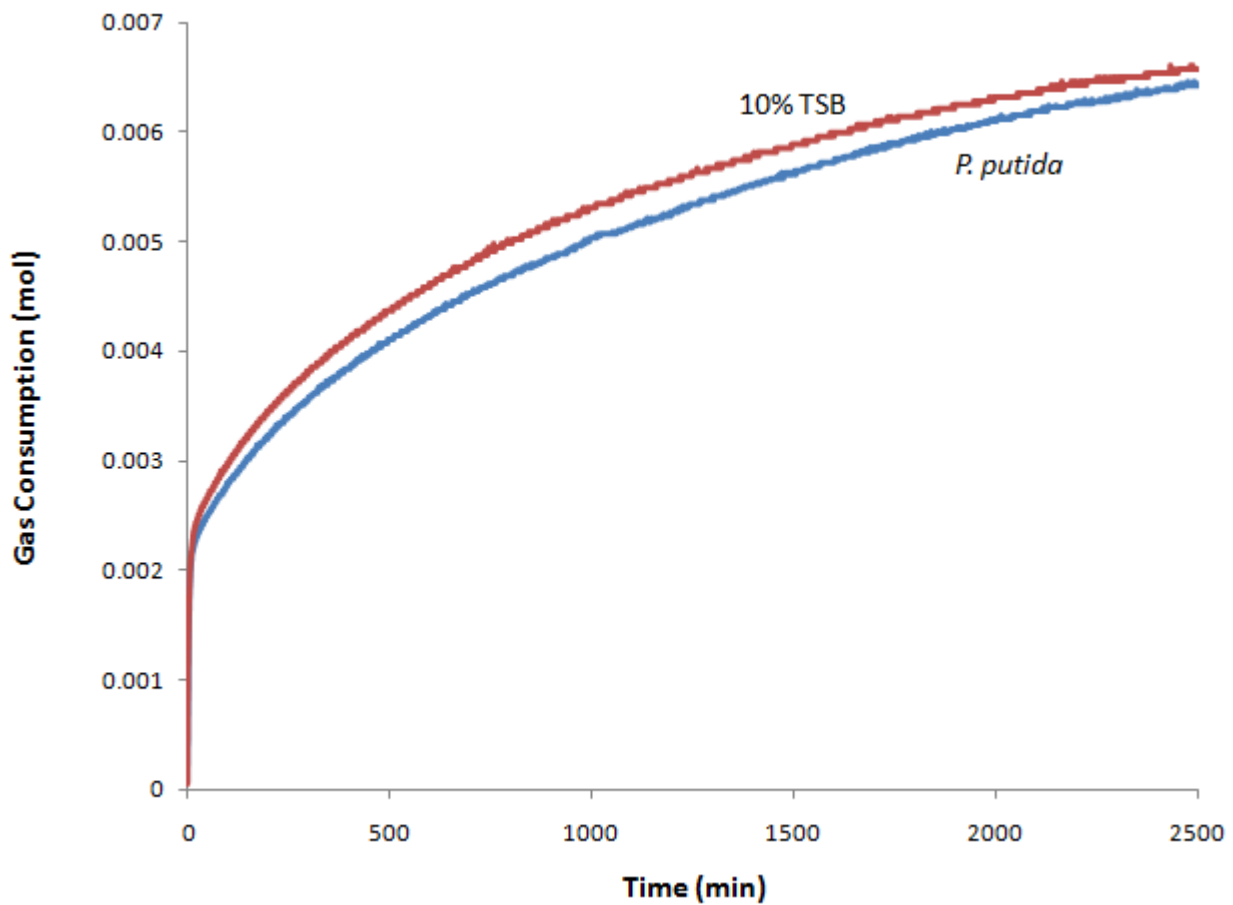


Figure 3.4. Methane/Ethane/Propane Gas Uptake. Gas consumption as hydrate forms from a solution of 400 million cells/ml *P. putida* UW4 in 10% TSB versus control 10% TSB. Total Gas consumption is proportional to the amount of hydrate formed.

Chapter 4

General Discussion

As the petroleum industry moves into more remote locations, where higher pressures and lower temperatures allow for hydrate formation to readily occur, problems such as pipeline blockage and damage as well as more serious cases of blowouts and personnel deaths have been reported as a result of hydrate growth.¹ For over five decades, polar solvents like glycols and methanol have been effectively used for preventing or controlling hydrate formation in these systems.² More recently, these thermodynamic inhibitors are being replaced by less environmentally-harmful and sometimes cheaper inhibitors, which include KI, polymers that inhibit nucleation and subsequent crystal growth of hydrates, and AAs, molecules with polar and non-polar groups that allow for the separation of the hydrocarbon-water phases, thus preventing further clustering of pre-existing hydrate particles.^{3,4} Nevertheless, there are limitations to these compounds, where KIs are not effective at higher driving forces nor for sour-gas applications, and AAs cannot function below watercuts of 30-40%.^{5,6} Presently, the search for more effective, cheaper and less toxic hydrate inhibitors continues.

This thesis contributes to the ongoing investigation of the association of ice-binding macromolecules with hydrates and their use as models for studying and developing biologically-based hydrate inhibitors.⁷

4.1. AFP binding and hydrate inhibition

A feature of KIs such as PVP is that they bind to the surface of hydrates and are believed to inhibit the formation of cages around the guest molecule.⁸ As a result, they have been shown

to modify crystal structures of sI ethylene oxide and sII THF hydrates and also delay nucleation in various high-pressure systems.⁹⁻¹¹ Using polycrystalline THF hydrate, I showed that GFP-tagged AFPs adsorbed to the surface of the hydrate and became adsorbed into the growing crystal (Chapter 2). Of the AFPs tested, more LpAFP-GFP appeared to adsorb to THF hydrate at the higher tested concentrations as opposed to Type III AFP-GFP, which adsorbed in higher molar quantities at lower concentrations. GFP by itself was found to be excluded from the growing crystal. While it is not surprising that GFP, which had no TH and no known ice-binding site, did not adsorb to hydrate, it was unexpected to find that LpAFP-GFP, a larger protein with a lower TH than Type III AFP-GFP, adsorbed to hydrate at a higher molar concentration. The reason for this observation is unknown. However, one possibility may be that LpAFP is less prone to denaturation in THF than Type III AFP. Although the beta-roll shaped LpAFP has been shown to be heat labile,¹² it is possible that this fold may allow it to be more structurally-intact in THF than the Type III AFP, which may unfold more easily due to its comparatively complex globular structure.¹³ Another possibility may be that at higher concentrations, when proteins are much closer together, certain structurally similar motifs can interact, such as the second flat binding face that is believed to be secondary ice-binding site on LpAFP.¹⁴ These protein-protein interactions can possibly allow LpAFP to form stacks on the hydrate surface, allowing for higher adsorption. Observations of AFP-hydrate inhibition using NMR has previously been documented,⁷ this technique can be used in order to obtain a more thorough understanding of LpAFP-hydrate binding characteristics.

When single THF hydrate crystals were grown in solutions containing AFP, similar morphological changes were observed to those grown in solutions with PVP (Chapter 2). Most notably, the interior sections of the {111} crystal faces formed in a skeletal or hopper shape,

indicative of reduced crystal growth rates as a result of interference in crystal formation (attributable to inhibitor binding) and generally lower levels of supercooling at these sites (due to the exothermic nature of crystal growth).¹⁵ This clearly indicates that like KIs, AFPs inhibit hydrate crystals using a similar binding-inhibition mechanism. At the lowest concentration (15 µg/ml), Type III AFP was the only additive to show well-defined skeletal growth of THF hydrate single crystals. Type III AFP-GFP showed deeper and more well-pronounced skeletal crystals than LpAFP-GFP at 200 µg/ml. GFP did not show major morphological changes. These effects could be attributed to the higher TH activities of Type III AFP and Type III AFP-GFP compared to LpAFP-GFP and GFP, indicating a similar TH-dependent inhibition mechanism to that of AFPs with ice.¹⁶ Analogous to the single crystal results, the same pattern was seen with the high-pressure methane/ethane/propane hydrate experiments, where Type III AFP was the most effective growth inhibitor, followed by Type III AFP-GFP, LpAFP-GFP and lastly GFP and PVP. Comparisons between high pressure and THF hydrate models show that AFPs can inhibit both hydrate systems and that THF hydrate, although a non-natural gas hydrate, serves as a good model for understanding gas hydrate-inhibitor interactions at the visible scale.

I believe that AFPs can use their ice binding sites, which normally fit with and bind to hexagonal ice,¹⁷ to bind to cubically-arrange ice-lattices. It should be noted that preferential binding to certain faces of ice are seen with AFPs,¹⁶ including LpAFP and Type III AFP. Since THF hydrate forms cubic crystals with 8 identical {111} faces,⁹ no preferential binding was observed nor expected. *In vitro* mutagenesis experiments have been able to detect AFP residues involved in ice-binding,¹⁸ similarly, this technique can be used to identify if the same residues are active in hydrate binding.

The AFPs used in this thesis proved successful in further understanding AFP-hydrate interactions (Chapter 2). There are nevertheless a multitude of other AFPs, many of which have higher activities than those used here,^{19,20} that if stable in THF, could be tested on polycrystalline and single crystal THF hydrate and/or in high-pressure systems with natural gas. Additionally, although Type III AFP was found to readily precipitate in THF (Chapter 2), further adsorption work with unmodified (GFP-tag deficient) AFPs may provide more effective inhibition, as noted from single crystal and high-pressure gas mix studies (Chapter 2), which compared Type III AFP and Type III AFP-GFP. GFP-tagged AFPs proved effective for observing protein adsorption to hydrates through fluorescence and may also prove useful for observing if and how AFPs adsorb to high-pressure hydrates. Polycarbonate high-pressure cells, which have shown to be useful for the visualization of pressurized gas hydrate growth,²¹ can be designed in order to visually detect if the AFPs are adsorbing and incorporating themselves into the growing hydrate, as well as any structural modifications to hydrate growth.

Since sII is the predominant form in hydrate plugs due to the presence of larger hydrocarbons like propane and butane,²² the major focus of this thesis was on sII hydrates. I nevertheless attempted to document any inhibitory effects of the GFP-tagged AFPs and control GFP on sI methane hydrate (Appendix A). It has previously been found that Type I AFP (from fish) inhibits methane hydrate similarly to PVP at low driving forces.⁷ Using GFP-tagged proteins, the LpAFP-GFP sample had the lowest gas consumption levels of the three proteins tested. Furthermore, LpAFP-GFP had unexpectedly delayed methane hydrate nucleation 14-fold compared to the control GFP, while Type III AFP-GFP did not show any such results. This observation is unlike that of LpAFP-GFP in the sII gas mix, where it proved inferior to Type III AFP-GFP in gas consumption inhibition. Nonetheless, nucleation delay was not observed in any

of the sII gas hydrate samples. It is not fully understood if the nucleation delay caused by LpAFP-GFP was a coincidence or as a result of its ability to more effectively inhibit sI over sII. Future tests will be required to compare with PVP and confirm the results are reproducible.

Further investigations into the inhibitory effects of AFPs on sI hydrates can further clarify the methane hydrate results and apart from methane hydrate, sI hydrates can also be made from ethylene oxide (EO). Similar to THF, when EO is mixed with water (7.7 H₂O:1 EO) it can form hydrate below 10°C.²³ This may prove useful for observing the effects of AFPs on sI crystal morphology and has previously been shown successful with KIs.⁹ EO vapor is nevertheless highly toxic and flammable, even in solution,²⁴ and precautions must be taken, such as maintaining clean equipment (acids, bases, metal oxides and salts and have shown to cause exothermic EO polymerization), wearing protective gear (safety goggles, butyl gloves) and handling EO and EO solutions strictly under a fume hood.

A theory for the superior nucleation inhibition of AFPs compared to PVP was developed by Zeng *et al.*²⁵ in order to interpret the data obtained using a QCM-D. Since AFPs like Type I bound better and formed denser aggregates on hydrophilic surfaces like amorphous silica it was suggested that this type of AFP can adhere to and block nucleation sites on particles or container walls.²⁵ My results obtained from QCM-D and quartz using GFP-tagged Type III or LpAFP did not show that these AFPs bound any better than control GFP (Appendix B). Further testing with non GFP-tagged proteins or other silica-based materials is proposed as well as GFP-tagged Type I AFP in order to understand these differences.

4.2. Cold-adapted bacteria and THF hydrate

Former work with cold-adapted bacteria such as *Chryseobacteria* sp. C14 appeared to show a nucleation delay and crystal shaping in THF hydrate.²⁶ Following the success with polycrystalline THF hydrate and AFPs, binding affinities of various cold-adapted bacteria to polycrystalline THF hydrate was tested (Chapter 3). The bacterial solutions usually became cloudy with THF present and proved very toxic to the organisms. Although at first it was believed THF may have caused cell lysis, further investigation showed that although the bacteria were unable to divide they were nevertheless intact. Some strains like *Chryseobacteria* sp. C14 and *E. coli* (BL21) became aggregated, and this was especially pronounced in the former. The reasons for this aggregation are unknown, but it has been suggested that the polar THF may cause changes in polarity of bacterial surface proteins, allowing them to aggregate as has been documented in solvent-exposed proteins.^{27,28}

Prior to testing for THF inhibition, amongst various salt and detergents, Triton X-100 was found to be most effective at treating aggregations seen with *Chryseobacteria* sp. C14 and *E. coli* cultures. Adsorption results showed that freeze-thaw resistant *Buttiauxella* G2b1 and *P. putida* UW4, noted to have ice-shaping proteins,²⁹ were able to bind to THF hydrate more effectively than *E. coli* and *Chryseobacteria* sp. C14, possibly as a result of cryoprotectants like ice-associating proteins, which are not found in bacteria like *E. coli*. *Chryseobacteria* sp. C14, is considered, but not formally shown to have AFP activity,³⁰ and this strain delayed nucleation in THF hydrate,²⁶ but did not bind THF hydrate (Chapter 2). This is possibly due to higher levels of aggregation, not seen in *Buttiauxella* sp. G2b1 or *P. putida* UW4.

Bacteria with ice-affinity have been selected and purified in a similar fashion using a cooled brass finger with ice.³¹ Likewise, our method with THF hydrate may also prove useful for selecting bacteria with prospective hydrate binding. If hydrate-binding selection is to be done from a consortium, due to THF toxicity, the adsorbed-bacteria/hydrate melts cannot be used to grow colonies for identification and selection purposes as previously done with ice.³¹ Nonetheless, gene sequencing of the adsorbed bacteria could allow for further identification and subsequent hydrate inhibition testing.

There was a correlation between bacterial adsorption and growth rate inhibition of THF hydrate. *Buttiauxella* sp. G2b1 and *P. putida* UW4 showed the most pronounced levels of adsorption and inhibition, with *P. putida* UW4 notably inhibiting THF hydrate growth up to 24%. Similarly, the *E. coli* and *Chryseobacteria* sp. C14 showed adsorption levels from 20 to 50% lower than the other strains and did not have such high inhibition levels. While *P. putida* UW4 proved effective with THF hydrate, it did not show significant inhibition with the high-pressure gas mix hydrate. It is hypothesized that the pore diameter of the silica gel used in these experiments was not large enough for the bacteria to enter inside. This may have allowed most of the water inside the silica gel to form hydrate as it was not in contact with the bacteria. Further tests may require silica gels with pore sizes $>20,000 \text{ \AA}$.

4.3. Concluding comments

In conclusion, for the first time documented, I have shown that ice-associating biologically-based macromolecules such as AFPs and cold-adapted bacteria have the ability to adsorb into structurally-distinct clathrate hydrates. Additionally, I have further shown that these materials can inhibit hydrate more effectively than a commercial KI (PVP) as well as non-

hydrate binding macromolecules. These results bring us closer to developing industrially-applicable microbial-based hydrate inhibitors that can potentially be used in the oil and gas industry.

References

1. Mehta, A., Walsh, J. and Lorimer, S. (2006) Hydrate Challenges in Deep Water Production and Operation. *Annals of the New York Academy of Sciences* **912**, 366-373.
2. Koh, A. C., Westacott, E. R., Zhang, W., Hirachand, K., Creek, L. J. and Soper, K. A. (2002) Mechanisms of gas hydrate formation and inhibition. *Fluid Phase Equilibria* **30**, 143-151.
3. Lederhos, P. L., Long, P. J., Sum, A., Christiansen, L. R. and Sloan Jr., D. E. (1996) Effective kinetic inhibitors for natural gas hydrates. *Chemical Engineering Science* **51**, 1221-1229.
4. Huo, Z., Freer, E., Lamar, M., Sannigrahi, B., Knauss, M. D. and Sloan Jr., D. E. (2001). Hydrate plug prevention by anti-agglomeration. *Chemical Engineering Science* **56**, 4979-4991.
5. Clark, L. W., Anderson, J., Barr, N. and Kremer, E. 2008. GUAP3 Scale Dissolver and Scale Squeeze Application Using Kinetic Hydrate Inhibitor (KHI). Proceedings of the 6th International Conference on Gas Hydrates (ICGH 2008), Vancouver, British Columbia, Canada, July 6-10, 2008.
6. Peytavy, J. L., Gleantm, P. and Bourgm, P. (2008) Qualification of Low Dosage Hydrate Inhibitors (LDHIs): Field Cases Studies Demonstrate the Good Reproducibility of the Results Obtained from Flow Loops. Proceedings of the 6th International Conference on Gas Hydrates (ICGH 2008) Vancouver, British Colombia, Canada, July 6-10, 2008.
7. Zeng, H., Wilson, D. L., Walker, K. V. and Ripmeester, A. J. (2006) Effect of Antifreeze Proteins on the Nucleation, Growth, and the Memory Effect during Tetrahydrofuran Clathrate Hydrate Formation. *Journal of American Chemical Society* **128**, 2844-2850.
8. Bjorn, K., Forrisdahl, G. and Kristian, O. (1997) Molecular dynamics simulations of PVP kinetic inhibitor in liquid water and hydrate/liquid water systems. *Molecular Physics* **90**, 979-992.
9. Larsen, R., Knight, A. C. and Sloan, D. E. (1998) Clathrate hydrate growth and inhibition. *Fluid Phase Equilibria* **150**, 353-360.
10. Moon, C., Taylor, C. P. and Rodger, M. P. (2003) Clathrate nucleation and inhibition from a molecular perspective. *Canadian Journal of Physics* **81**, 451-457.
11. Jensen, L., Thomsen, K. and von Solms, N. (2008) Propane hydrate nucleation: Experimental investigation and correlation. *Chemical Engineering Science* **63**, 3069-3080.
12. Sidebottom, C., Buckley, S., Pudney, P., Twigg, S., Jarman, C., Holt, C., Telford, J., McArthur, A., Worrall, D., Hubbard, R. and Lillford, P. (2000) Phytochemistry: Heat-stable antifreeze protein from grass. *Nature* **406**, 256.

13. Antson, A. A., Smith, J. D., Roper, I. D., Lewis, S., Caves, D.S. L., Verma, S.C., Buckley, L. S., Lillford, J. P., Hubbard, E. R. (2001) Understanding the mechanism of ice binding by type III antifreeze proteins. *Journal of Molecular Biology* **305**, 875-889.
14. Middleton, J. A., Brown, M. A., Davies, L. P. and Walker, K. V. (2009) Identification of the ice-binding face of a plant antifreeze protein. *Federation of the Societies of Biochemistry and Molecular Biology Letters* **583**, 815-819.
15. Knight, A.C. and Rider, K. (2002) Free-growth forms of tetrahydrofuran clathrate hydrate crystals from the melt: plates and needles from a fast-growing vicinal cubic crystal. *Philosophical Magazine A* **82**, 1609-1632.
16. Scooter, J. A., Marshall, C. B., Graham, A. L., Gilbert, A. J., Garnham, P. C. and Davies, L. P. (2006) The basis for hyperactivity of antifreeze proteins. *Cryobiology* **53**, 229-239.
17. Materer, N., Starke, U., Barbieri, M., van Hove, A., Somorjai, G. A., Kroes, J. G. and Minot, C. (1995) Molecular Surface Structure of a Low-Temperature Ice Ih(0001) Crystal. *Journal of Physical Chemistry* **99**, 6267-6269.
18. Tyshenko, G. M., Doucet, D., Davies, L. P. and Walker, K. V. (1997) The antifreeze potential of the spruce budworm thermal hysteresis protein. *Nature* **15**, 887-890.
19. Marshall, B. C., Fletcher, L. G. and Davies, L. P. (2004) Hyperactive antifreeze protein in a fish. *Nature* **429**, 153.
20. Qin, W. and Walker, V.K. (2006) Tenebrio antifreeze protein gene identification and regulation. *Gene* **367**, 142-149.
21. Rehder, G., Kirby, H. S., Durham, B. W., Stern, A. L., Peltzer, T. E., Pinkston, J. and Brewer, G. P. (2004) Dissolution rates of pure methane hydrate and carbon-dioxide hydrate in undersaturated seawater at 1000-m depth. *Geochimica et Cosmochimica Acta* **68**, 285-292.
22. Davies, R. S., Selim, S. M., Sloan, D. E., Bollavaram, P. and Peters, J. D. (2006) Hydrate Plug Dissociation. *American Institute of Chemical Engineers Journal* **52**, 4016.
23. Huo, Z., Jager, D. M., Miller, T. K. and Sloan, D. E. (2002) Ethylene oxide hydrate non-stoichiometry: measurements and implications. *Chemical Engineering Science* **57**, 705-713.
24. Ethylene Oxide; MSDS No. G90; BOC Gases, Murray Hill, NJ, 1996.
25. Zeng, H., Lu, H., Huva, E., Walker, K. V. and Ripmeester, A. J. (2007) Differences in nucleator adsorption may explain distinct inhibition activities of two gas hydrate kinetic inhibitors. *Chemical Engineering Science* **63**, 4026-4029.

26. Huva, Emily I.; Gordienko, Raimond V.; Ripmeester, John A.; Zeng, Huang; Walker, Virginia K. 2008. The Search for “Green Inhibitors”: Perturbing Hydrate Growth with Bugs. Proceedings of the 6th International Conference on Gas Hydrates, Vancouver, BC, Canada, July 6-10, 2008.
27. Sugunakar, Y. and Przybycien, M. (1996) Simulations of Reversible Protein Aggregate and Crystal Structure. *Biophysical Journal* **70**, 2888-2902.
28. Tartaglia, G. G., Cavalli, A., Pellarin, R. and Caflisch, A. (2004) The role of aromaticity, exposed surface, and dipole moment in determining protein aggregation rates. *Protein Science* **13**, 1939-1941.
29. Cheng, Z. Park, E. and Glick, R. B. (2007) 1-Aminocyclopropane-1-carboxylate deaminase from *Pseudomonas putida* UW4 facilitates the growth of canola in the presence of salt. *Canadian Journal of Microbiology* **53**, 912-918.
30. Walker, K. V., Palmer, R. G. and Voordouw, G. (2006) Freeze-Thaw Tolerance and Clues to the Winter Survival of a Soil Community. *Applied and Environmental Microbiology* **72**, 1784-1792.
31. Wilson, S., Kelley, D. L. and Walker, K. V. (2006) Ice-active characteristics of soil bacteria selected by ice-affinity. *Environmental Microbiology* **8**, 1816-1824.

Summary

1. LpAFP-GFP and Type III AFP-GFP were found to adsorb to polycrystalline THF hydrate while control GFP did not (Chapter 2).
2. The tested AFPs inhibited the normal growth of single-crystal THF hydrate and formed hopper crystals (Chapter 2).
3. The tested AFPs inhibited the growth of high-pressure natural gas hydrate more effectively than GFP and PVP with Type III AFP showing the greatest crystal shaping (at 15 $\mu\text{g/ml}$) and the best gas hydrate inhibition (at 0.1 mM) (Chapter 2).
4. The cold-adapted bacteria *Buttiauxella* sp. G2b1 and *P. putida* UW4 adsorbed at higher levels and had more pronounced inhibitory effects on THF hydrate growth rates compared with *E. coli* BL21 and *Chryseobacteria* sp. C14 (Chapter 3).
5. *P. putida* UW4 inhibited the formation of high-pressure natural gas hydrate, although to a lesser degree than in THF hydrate (Chapter 3).
6. LpAFP-GFP showed inhibition of sI methane hydrate (Appendix A).
7. LpAFP-GFP and Type III AFP-GFP did not appear to adsorb more tightly to silica or quartz compared to GFP (Appendix B).

Appendix A

AFPs and sI Methane Hydrate

Raimond Gordienko*, Robin Susilo†, Virginia K. Walker* and John Ripmeester†.

Departments of Biology*, Queen's University, Kingston ON, K7L 3N6, Canada. Materials Structure and Function Group†, National Research Council Canada, Ottawa ON, K1A 0R6, Canada.

Abstract

The recombinant plant antifreeze protein (AFP) from *Lolium perenne* (LpAFP-GFP) was found to delay nucleation and lead to lower levels of hydrate formation compared with fish Type III AFP-GFP and control GFP. Because of the lack of evidence that LpAFP-GFP is a more effective hydrate inhibitor than Type III AFP-GFP using sII hydrates, it is not known if these results are due to LpAFP-GFPs preferential inhibition of sI over sII, the lower driving pressure or the stochastic nature of nucleation.

Introduction

Structure II (sII) hydrates are the most predominant forms in gas hydrate plugs.¹ Nevertheless, structure I (sI) hydrates, notably methane hydrate, occur in large abundance in the Arctic and undersea sediments, and are believed to hold over half the world's fossil fuel reserve as enclathrated methane.² Antifreeze proteins (AFPs) from the ryegrass (*Lolium perenne* AFP; LpAFP-GFP) and ocean pout (*Zoarces americanus*; Type III AFP-GFP) have proved successful

in inhibiting sII tetrahydrofuran (THF) and may be useful for methane/ethane/propane (gas mix) hydrates (Chapter 2). As a result, we tested these proteins on sI methane hydrate.

Methods/Results

Methane hydrate experiments were performed in the system used previously for sII gas mix hydrates (Chapter 2). The recombinant proteins LpAFP-GFP, Type III AFP-GFP and control GFP, produced in a bioreactor a previously illustrated (Chapter 2), were mixed separately at 55 μ M with silica gel and loaded into a high-pressure cell that was purged twice and pressurized to 40 bar (580 PSI) with methane gas (>99%, Linde Canada, Mississauga, ON). They were placed in a water bath at 0.5°C to initiate hydrate nucleation. A sudden drop in pressure was used to indicate hydrate nucleation and gas consumption was calculated as previously described (Chapter 2).

Delays in nucleation were notably observed with the LpAFP-GFP sample (Fig. A.1), which showed a >14-fold delay in methane hydrate nucleation over the control GFP. Additionally, when the LpAFP-GFP was used, the lowest level of hydrate formed, indicated by the lowest calculated gas consumption value of 16.6 mmol. Conversely, when compared with the control GFP, Type III AFP-GFP only delayed methane hydrate by <1.1-fold and consumed 17.6 mmol of gas, lower only than the 18.5 mmol consumed by the GFP sample. The pressure trends in Fig. A.1 also indicate there was no general reduction in the growth rate of methane hydrate formation between the samples, as seen by the steep pressure drops following nucleation.

Discussion

While LpAFP-GFP did not inhibit sII gas mix hydrate growth as well as Type III AFP-GFP (Chapter 2), it proved more effective in sI methane hydrate (Fig. A.1). The reasons for the divergence in results between the two tested hydrates are not fully understood. Though the antifreeze activity (thermal hysteresis) of LpAFP-GFP is lower than Type III AFP-GFP (Chapter 2), the lower levels of hydrate formation in the LpAFP-GFP sample may be due to LpAFP-GFPs ability to effectively allow smaller ice crystals to remain small and not grow to larger, more thermodynamically-favorable crystals, a property known as ice-recrystallization inhibition.³

While this was not previously observed in the sII gas mix hydrate, the lower driving pressure used in the methane hydrate samples could also have allowed the LpAFP-GFP to function more effectively (AFPs have shown improved hydrate inhibition at lower driving forces).⁴ sI and sII both form cubic crystals, and both LpAFP-GFP and Type III AFP-GFP have shown to be able to inhibit the crystal growth of sII tetrahydrofuran hydrate (Chapter 2), the possibility that LpAFP-GFP can inhibit sI hydrate more effectively is a consideration, although more studies must be performed to verify this view. Lastly, hydrate nucleation is stochastic,⁵ and the large nucleation delay seen by the LpAFP-GFP sample may have been due to chance; future nucleation trials may require larger sample sizes.

In conclusion, it is not known if the nucleation and formation inhibition of sI hydrate by LpAFP-GFP is due to the stochastic nature of nucleation, driving pressure or the preferential inhibition of sI over sII. Larger sample sizes and comparisons with commercial kinetic hydrate inhibitor, poly-N-vinylpyrrolidone (PVP), must be performed in future experiments to further validate these observations.

References

1. Davies, R. S., Selim, S. M., Sloan, D. E., Bollavaram, P. and Peters, J. D. (2006) Hydrate Plug Dissociation. *American Institute of Chemical Engineers Journal* **52**, 4016.
2. Lee, S. and Holder, D. G. (2001) Methane hydrates potential as a future energy source. *Fuel Processing Technology* **71**, 181-186.
3. Sidebottom, C., Buckley, S., Pudney, P., Twigg, S., Jarman, C., Holt, C., Telford, J., McArthur, A., Worrall, D., Hubbard, R. and Lillford, P. (2000) Phytochemistry: Heat-stable antifreeze protein from grass. *Nature* **406**, 256.
4. Al-Adel, S., Dick, G. A. J., El-Ghafari, R. and Servio, P. (2008) The effect of biological and polymeric inhibitors on methane gas hydrate growth kinetics. *Fluid Phase Equilibria* **267**, 92-98.
5. Natarajan, V., Bishnoi, R. P. and Kalogerakis, N. (1994) Induction phenomena in gas hydrate nucleation, *Chemical Engineering Science* **49**, 2075–2087.

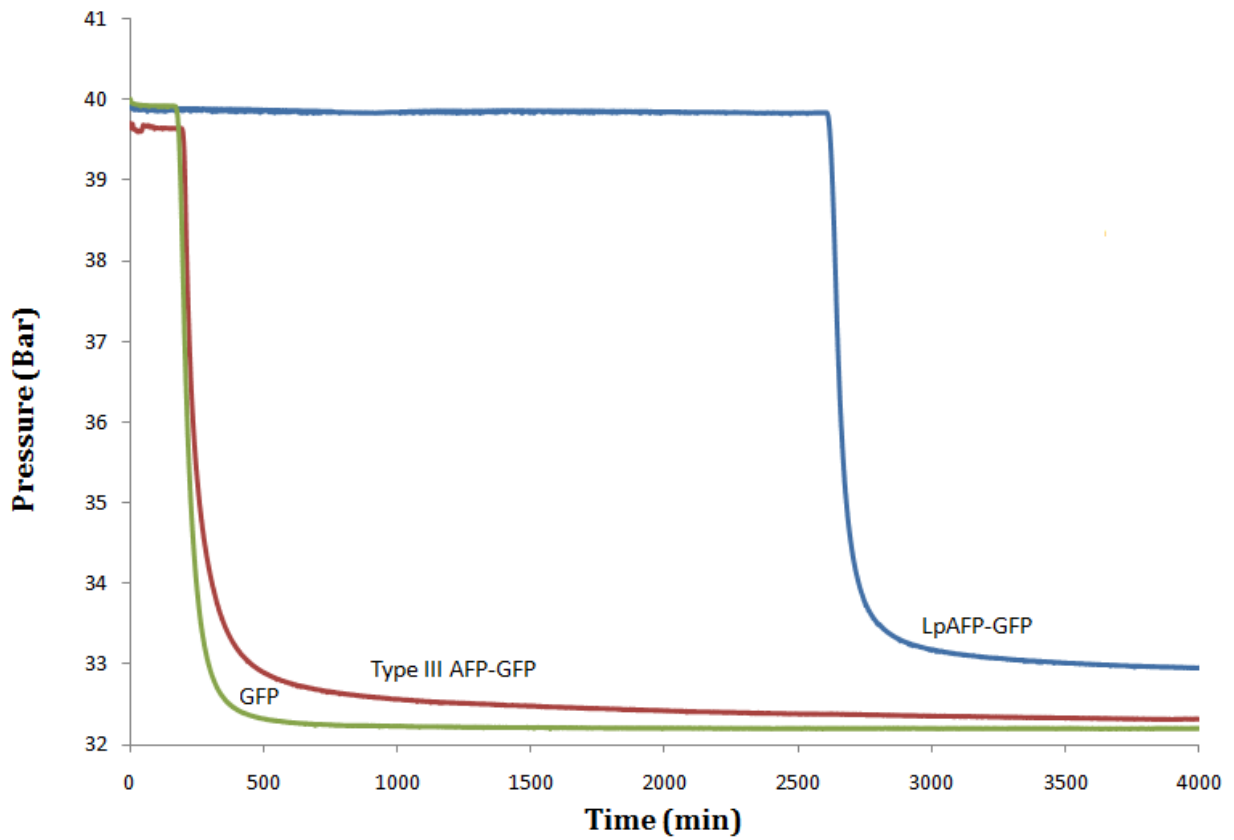


Figure A.1. Pressure trends for methane hydrate. Points where sudden pressure drops are seen indicate hydrate nucleation. Absolute pressure drops are proportional to gas consumption levels, which are indicative of amounts of enclathrated methane.

Appendix B

AFP Adsorption Studies with Amorphous Silica and Quartz

Raimond Gordienko*, Virginia K. Walker* and John Ripmeester†.

Departments of Biology*, Queen's University, Kingston ON, K7L 3N6, Canada. Materials Structure and Function Group†, National Research Council Canada, Ottawa ON, K1A 0R6, Canada.

Abstract

Hydrophilic particles and surfaces have been proposed as sites for hydrate nucleation. The adsorption of hydrophilic molecules such as antifreeze proteins (AFPs) onto these surfaces is believed to reduce rate of hydrate nucleation. Work with the Quartz Crystal Microbalance with Dissipation (QCM-D) has shown that spruce budworm and winter flounder AFPs can bind to amorphous silica with more affinity than kinetic hydrate inhibitor poly-N-vinylpyrrolidone (PVP). Our results show that green fluorescent protein (GFP)-tagged AFPs from *Lolium perenne* (LpAFP-GFP) and fish (Type III AFP-GFP) have no higher affinity towards amorphous silica than the control GFP. Additionally, we found that PVP did not adsorb to amorphous silica and Type III AFP-GFP did not show enhanced binding to quartz. The results indicate that although hydrophilic in nature, amorphous silica and quartz cannot serve as binding sites for AFPs tested here.

Introduction

The presence of hydrophilic particles and solid surfaces, such as container walls, likely serve as nucleating sites for hydrates in oil and gas pipelines and therefore limiting the formation of embryonic hydrate structures on nucleating sites should reduce overall hydrate formation in a system.^{1,2} To understand the kinetics of molecular interactions at a liquid-solid interface, a Quartz Crystal Microbalance with Dissipation (QCM-D) has been used.³ QCM-D measures adsorbent mass (through changes in frequency) and viscoelasticity, or shear-stress (termed dissipation) of adsorbent molecules onto piezoelectric crystals coated with either hydrophilic or hydrophobic material which interacts with the adsorbent.⁴ It has previously been found that spruce budworm and winter flounder bind to hydrophilic amorphous silica more effectively than the commercial kinetic hydrate inhibitor poly-N-vinylpyrrolidone (PVP).⁵ Such binding could also allow these AFPs to block nucleation sites of solid hydrophilic particles or structures which may cause a delay in hydrate nucleation. In an attempt to determine if the LpAFP-GFP and Type III AFP-GFP showed similar silica-binding capabilities, we tested their capacity to bind to amorphous silica as well as crushed α -quartz crystals.

Materials/Methods

QCM-D

Sample measurements of recombinant 30 μ M and 50 μ M green-fluorescent protein (GFP), GFP-tagged *Lolium perenne* AFP (LpAFP-GFP) and ocean pout Type III AFP (Type III AFP -GFP) or PVP (MW 10,000; Sigma-Aldrich, St. Louis, MO, USA) were performed with a QCM-D (Q-Sense D300, Q-Sense AB, Gothenburg, Sweden) as described by Zeng *et al.*⁵ Using 5-MHz AT-cut crystals coated with amorphous silica, the frequency (f) and dissipation (D)

values were recorded (Fig. B.1). Prior to experimentation, the crystals were cleaned in a solution of 10% sodium dodecyl sulphate, rinsed with water, dried with nitrogen gas and placed in a UV chamber for 10 min. The crystals were then loaded in the QCM-D measurement chamber with the silica-coated side facing the testing solution. Before the testing solution was introduced to the crystal, the temperature of the measuring cell was set to 15°C (the lowest possible setting) and purified water was used to wash the crystal until stable frequency and dissipation baseline values were achieved. Next, ~0.5 ml of the sample was added into the measurement chamber and changes in frequency and dissipation were recorded at 14.9 Hz. To observe the effects of washes on the samples, three washes (0.5 ml volumes per wash) were performed using 0.1M Tris/HCl (pH 8) after baseline levels of f and D were observed following sample addition.

Quartz Crystals

Macrocrystalline α -quartz (17.2 g total), which is known to be hydrophilic,⁶ was cleaned using acetic acid (pH 2.4), autoclaved, and incubated in 1.1 mg/ml solutions of Type III AFP-GFP and GFP. Protein adsorbance (visually detected via fluorescence) was determined by subsequently washing the crystals in 0.1 M Tris/HCl (pH 8) and placing them under UV light (302 nm). Macrocrystalline α -quartz were washed as described, crushed and ground, using a mortar and pestle, and sifted using a No. 60 sifter (250 μ m diameter). The sifted quartz powder was then autoclaved and incubated with 1.1 mg/ml concentrations of Type III AFP or GFP for 5 h with gentle mixing at 4°C. This protein-quartz mixture was then loaded into a 100 ml column and drained. To observe any protein/quartz binding-affinity, the quartz was washed with 8 ml solutions of 0.1 M Tris/HCl, pH 8 and pH 1.3, the flow-through was collected in 1.5 ml

microcentrifuge tubes at a 0.5 ml/min. The collected samples (10 μ l) from each tube were then electrophoresed on a 12% SDS-PAGE gel to observe protein elution as a result of washing.

Results/Discussion

As described by Zeng *et al.*,⁵ AFPs from the spruce budworm and winter flounder form compact films (higher D -values) on silica compared to PVP, while PVP had a larger adsorption mass (higher f -values), meaning a greater number of molecules bound at any given time. Our results with the QCM-D (Table 1) did not show that PVP bound at any comparable level at the concentrations tested (30 and 50 μ M). Surprisingly, at both concentrations, GFP appeared to have the largest adsorption mass and formed the most compact films (able to withstand more shear-stress) on the silica surface compared to the AFP-GFPs. At both concentrations, LpAFP-GFP had the highest adsorption mass and compact layers of the two AFP-GFPs. For both AFP samples, the washes did very little to change the f and D -values, indicating that the proteins were tightly bound to silica. Nevertheless, Type III AFP-GFP showed the largest disruptions in f and D -values during the washes. Unlike results obtained by Zeng *et al.*,⁵ our data indicate that PVP does not bind to amorphous silica and that although AFP-GFPs do, they generally show less adsorption (low f -values) and are more prone to shear-stress (higher D -values) than the control GFP. Because the temperature used in these tests was 15°C, the AFPs may not have been able to function at their normal temperature ranges of 0°C,⁷ this may explain the results, although why PVP showed no binding remains unknown.

Using 1.1 mg/ml Type III AFP-GFP on whole-crystal quartz showed no better adherence than GFP at the same concentration. When observed under the UV light, following one wash with 0.1 M Tris/HCl (pH 8) at 4°C, the proteins both washed off the crystals and no fluorescence

was detected (not shown). Washing the protein-incubated crushed quartz with solutions of 0.1 M Tris/HCl pH 8 and pH 1.3 (Figs. B.2.A and B.2.B), also showed similar elution patterns between Type III AFP-GFP and GFP. These results indicate no difference in quartz-affinity between the two proteins.

In conclusion, the AFPs did not bind appreciably to any of the silicon-based materials. Future experiments with non-GFP tagged AFPs at lower temperatures (although not possible for the QCM-D) and with different silicon-based materials and improved methods may prove more successful.

References

1. Sloan, D. E. and Koh, A. C. (2007) Clathrate Hydrates of Natural Gases, 3rd Ed. Fl: CRC Press.
2. Zeng, H., Walker, K. V. and Ripmeester A. J. (2007) Approaches to the Design of Better Low-Dosage Gas Hydrate Inhibitors. *Angewandte Chemie International Edition* **46**, 5402-5404.
3. Dejardin, P. (2006) Proteins at Solid-Liquid interfaces, 1st Ed. Springer. Germany: Springer-Verlag Berlin Heidelberg.
4. Feldoto, Z., Pettersson, T. and Dedinaite, A. (2008) Mucin-Elctrolyte Interctions at the Solid-Liquid Interface Probed by QCM-D. *Langmuir*, **24**, 3348-3357.
5. Zeng, H., Lu, H., Huva, E., Walker, K. V. and Ripmeester, A. J. (2007) Differences in nucleator adsorption may explain distinct inhibition activities of two gas hydrate kinetic inhibitors. *Chemical Engineering Science* **63**, 4026-4029.
6. Tarasevich, I. Y. (2007) The surface energy of hydrophilic and hydrophobic adsorbents. *Colloid Journal* **69**, 212-220.
7. Li, X., Trinh, K.Y., and Hew, C.L. 1991. Expression and characterization of an active and thermally more stable recombinant antifreeze polypeptide from ocean pout, *Macrozoarces americanus*, in *Escherichia coli*: Improved expression by the modification of the secondary structure of the mRNA. *Protein Eng.* 4: 995–1002.

| Additive | Δf 30 μ M | Δf 30 μ M Wash 1-3 | ΔD 30 μ M | ΔD 30 μ M Wash 1-3 | Δf 50 μ M | Δf 50 μ M Wash 1-3 | ΔD 50 μ M | ΔD 50 μ M Wash 1-3 |
|--------------|-----------------------|-----------------------------------|-----------------------|-----------------------------------|-----------------------|-----------------------------------|-----------------------|-----------------------------------|
| LpAFP-GFP | 159 | 0.920 | 4.69 | 0.705 | 205 | 0.460 | 5.75 | 0.341 |
| Type III GFP | 141 | 6.06 | 2.30 | 1.03 | 174 | 3.12 | 2.86 | 0.766 |
| GFP | 328 | 5.88 | 8.12 | 0.568 | 342 | 7.24 | 8.52 | 1.28 |
| PVP | N/A | N/A | N/A | N/A | N/A | N/A | N/A | N/A |

Table 1. Changes in frequency and dissipation for various additives. Changes in frequency (Δf , Hz) and dissipation (ΔD , $\times 10^{-6}$) measured at 30 and 50 μ M. Δf and ΔD were also measured from wash 1 to wash 3.

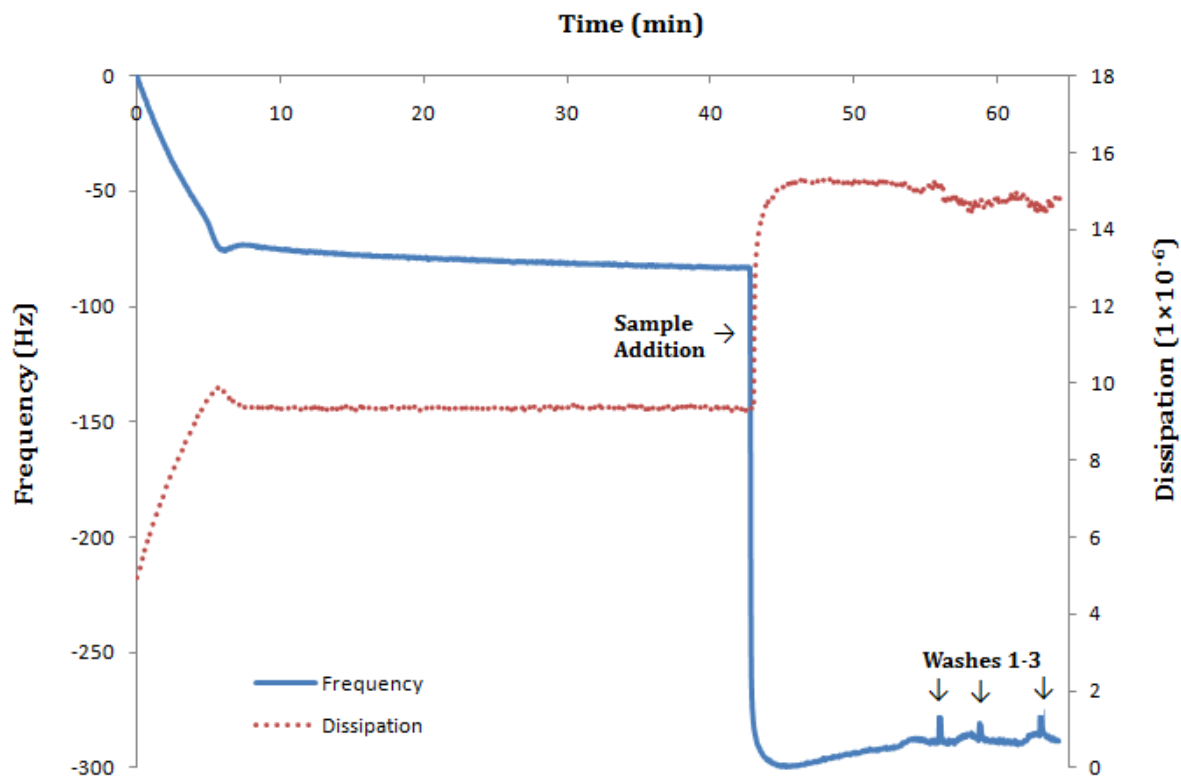


Figure B.1. Typical QCM-D frequency (f) and dissipation (D) trends. When baseline values of f and D are observed the sample is then added, this is followed by a sudden drop in frequency and rise in dissipation, afterwards the sample is washed three times with 0.1 M Tris/HCl (pH 8).

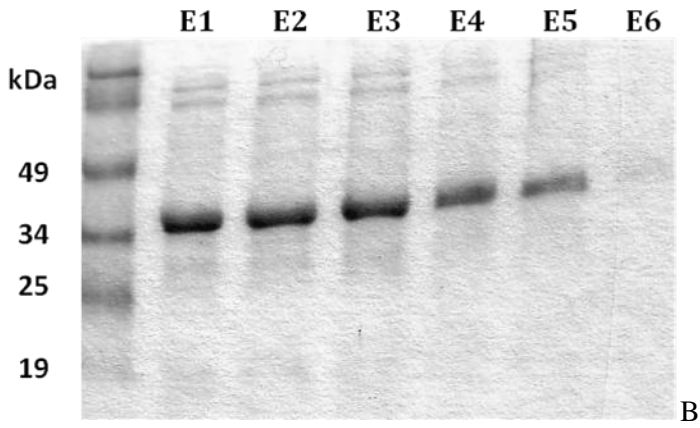
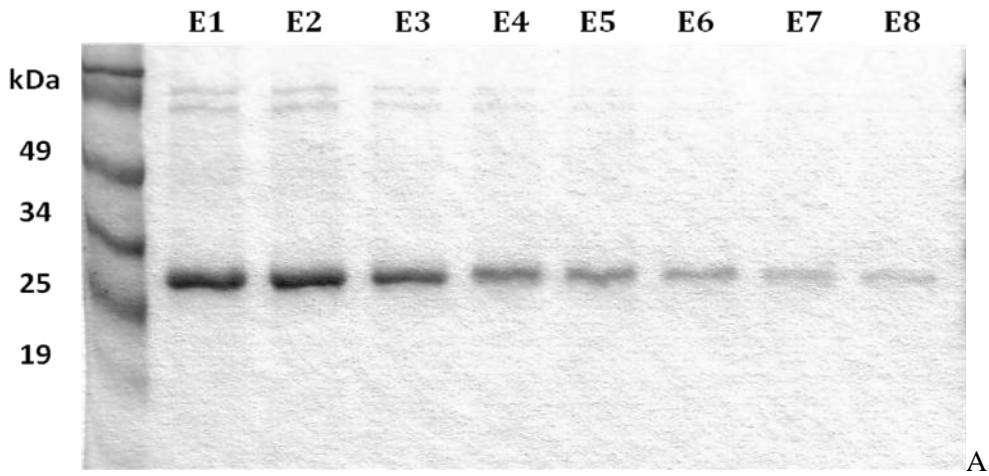


Figure B.2.A. Protein elution from quartz with 0.1 M Tris/HCl (pH 8). GFP (above) and Type III AFP-GFP (below) showed similar elution trends, where most of the protein eluted within 5 to 6 washes.

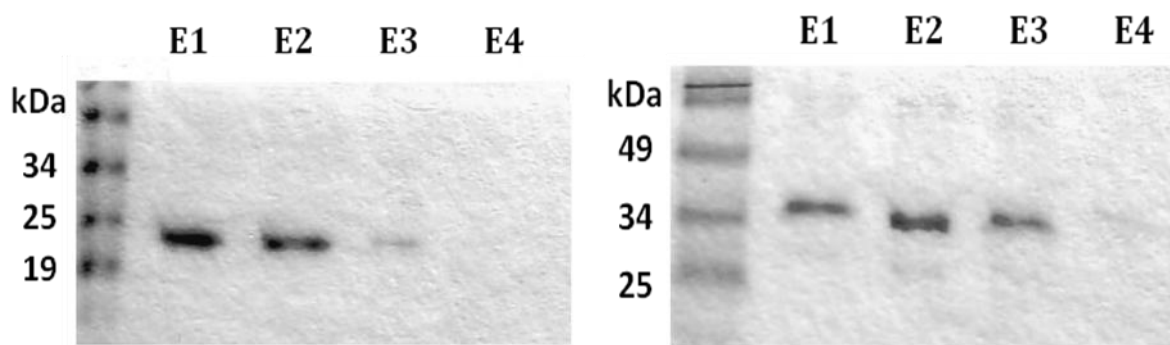
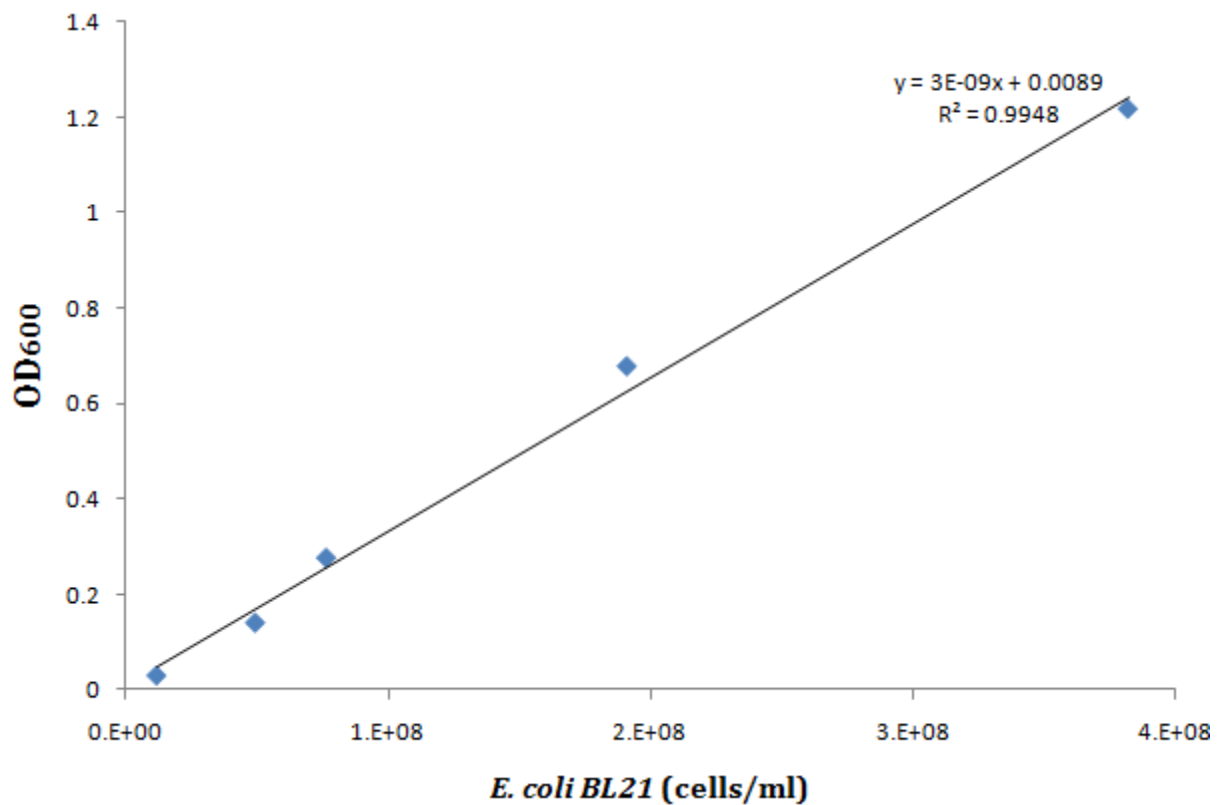
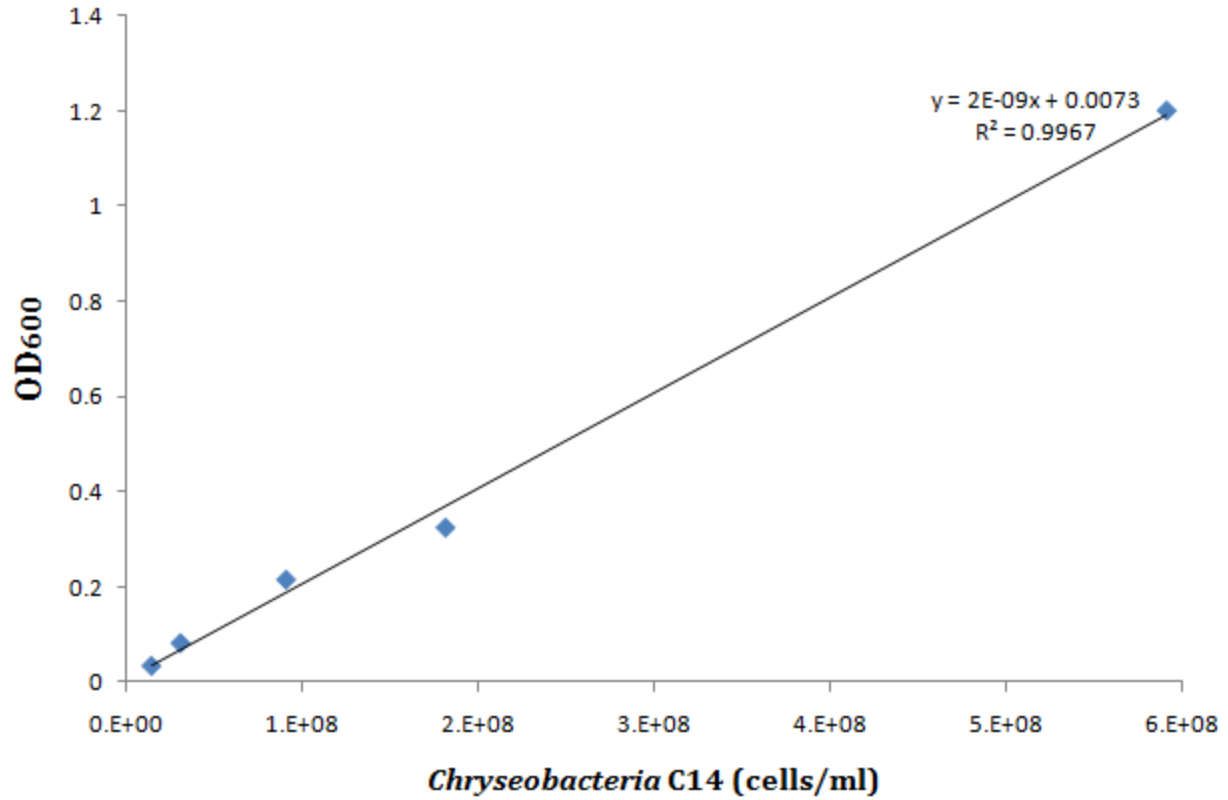


Figure B.2.B Protein elution from quartz with 0.1 M Tris/HCl (pH 1.3). GFP (left) and Type III AFP-GFP (right) showed similar elution trends, where most of the protein eluted within 3 washes.

Appendix C.1. Bacterial standard curves. Optical density at 600nm (OD600) vs. cell count.



Appendix C.2. Bacterial standard curves. Optical density at 600nm (OD600) vs. cell count.

